Multidetector CT of Blunt Cervical Spine Trauma in Adults[1]

David Dreizin, MD
Michael Letzing, MD
Clint W. Sliker, MD
Falgun H. Chokshi, MD
Uttam Bodanapally, MD
Stuart E. Mirvis, MD
Robert M. Quencer, MD
Felipe Munera, MD

A number of new developments in cervical spine imaging have transpired since the introduction of 64-section computed tomographic (CT) scanners in 2004. An increasing body of evidence favors the use of multidetector CT as a stand-alone screening test for excluding cervical injuries in polytrauma patients with obtundation. A new grading scale that is based on CT and magnetic resonance (MR) imaging findings, the cervical spine Subaxial Injury Classification and Scoring (SLIC) system, is gaining acceptance among spine surgeons. Radiographic measurements described for the evaluation of craniocervical distraction injuries are now being reevaluated with the use of multidetector CT. Although most patients with blunt trauma are now treated nonsurgically, evolution in the understanding of spinal stability, as well as the development of new surgical techniques and hardware, has driven management strategies that are increasingly favorable toward surgical intervention. It is therefore essential that radiologists recognize findings that distinguish injuries with ligamentous instability or a high likelihood of nonfusion that require surgical stabilization from those that are classically stable and can be treated with a collar or halo vest alone. The purpose of this article is to review the spectrum of cervical spine injuries, from the craniocervical junction through the subaxial spine, and present the most widely used grading systems for each injury type.

Abbreviations: MIP = maximum intensity projection, MVC = motor vehicle collision, NEXUS = National Emergency X-Radiography Utilization Study, SLIC = Subaxial Injury Classification and Scoring

RadioGraphics 2014; 34:1842–1865

Published online 10.1148/rg.347130094

Content Codes: CT ER MK NR

[1]From the Department of Diagnostic Radiology, University of Maryland Medical Center, R Adams Cowley Shock Trauma Center, 22 S Greene St, Baltimore, MD 21201 (D.D., C.W.S., U.B., S.E.M.); Department of Diagnostic Radiology, University of Miami Leonard Miller School of Medicine, Ryder Trauma Center, Jackson Memorial Hospital, Miami, Fla (M.L., R.M.Q., F.M.); and Department of Radiology, Emory University School of Medicine, Atlanta, Ga (F.H.C.). Recipient of a Cum Laude award for an education exhibit at the 2010 RSNA Annual Meeting. Received October 7, 2013; revision requested January 22, 2014, and received February 2; accepted March 25. For this journal-based SA-CME activity, the authors, editor, and reviewers have disclosed no relevant relationships. **Address correspondence to** D.D. (e-mail: *daviddreizin@gmail.com*).

SA-CME LEARNING OBJECTIVES

After completing this journal-based SA-CME activity, participants will be able to:

- Discuss the role of 64-section CT for excluding unstable cervical spine injury in polytrauma patients with obtundation.
- Describe the commonly used grading systems for injuries involving the occipital condyles, atlas, axis, and subaxial cervical spine.
- List the three separately graded components used to determine the SLIC score and the need for surgical stabilization.

See www.rsna.org/education/search/RG.

TEACHING POINTS

See last page

Introduction

Cervical spine injuries occur in 5%–10% of patients with blunt polytrauma. Of the approximately 10,000 spinal cord injuries that are diagnosed each year, 55% involve the cervical spinal cord. The estimated yearly cost for treating quadriplegic patients in the United States approaches $5.6 billion (1–3).

Multidetector computed tomography (CT) is used throughout major U.S. trauma centers as the initial screening examination for high-risk patients who are suspected of having cervical spine trauma, and multidetector CT is increasingly incorporated into whole-body CT protocols in the evaluation of blunt polytrauma. Radiologists can provide added value to their traumatology colleagues by developing an evidence-based understanding of the role

Table 1: Low-Risk Criteria for Clinical Exclusion of Cervical Spine Injury in Alert Stable Patients

NEXUS criteria
No posterior midline cervical tenderness
No intoxication
No focal neurologic deficit
No painful distracting injuries
Canadian C-spine rule criteria
Age < 65 years
No dangerous mechanism, such as:
Fall from height of >91 cm (>3 ft)
Axial loading injury (eg, diving accident)
High-speed motor vehicle collision (MVC) (>100 km/h), rollover, or ejection
Recreational motor vehicle, motorcycle, or bicycle injury
No paresthesias
Sitting position in emergency department
Ambulatory at any time
Neck rotation of 45° left and right

of multidetector CT in *(a)* evaluating the cervical spine in alert polytrauma patients and those with obtundation, *(b)* assessing the stability of cervical spine injuries, and *(c)* determining when surgical intervention is necessary. A high degree of suspicion based on a dangerous mechanism of injury or a neurologic injury should flag a cervical spine that appears normal at initial inspection for careful appraisal. Identification of cervical spine injury should trigger imaging of the remaining spinal axis because noncontiguous injuries occur in 10%–15% of cases (4,5). An awareness of *(a)* the limitations and blind spots of multidetector CT, *(b)* the appearance of normal variants, and *(c)* the complementary role of magnetic resonance (MR) imaging in determining injury severity and surgical approach is needed.

The purpose of this article is to describe the role of multidetector CT for screening and diagnosis of cervical spine trauma in adults. First, the concept of cervical spine "clearance" is explained, followed by a discussion of technique. Then various types of cervical spine injuries are described, from the craniocervical junction through the subaxial cervical spine. Finally, the limitations of multidetector CT, as well as normal variants and pitfalls, are discussed.

Cervical Spine Clearance

Asymptomatic Patients

Airway protection and cervical spine immobilization are the first steps of the Advanced Trauma Life Support protocol developed by the American College of Surgeons Committee on Trauma (6). After blunt trauma, the cervical spine should be considered injured until proven otherwise. Before cervical spine precautions can be safely removed, the cervical spine must be effectively excluded from injury, or "cleared."

In this article, *clearance* refers to the confident exclusion of unstable cervical spine injuries that could otherwise result in neurologic injury or death. Since the establishment of low-risk criteria by the Canadian C-spine rule study (7) and the National Emergency X-Radiography Utilization Study (NEXUS) (8) (Table 1), clearance of the cervical spine on clinical grounds alone has become the standard of care in alert adult patients with no midline cervical tenderness, neurologic symptoms, or distracting injuries (8). In the NEXUS study, fractures were missed in only eight of 818 cases by using their clinical decision tool, with a negative predictive value of 99.8% (8). The Canadian cervical spine clinical prediction rule (7) excluded cervical spine injury with 100% sensitivity in 8924 adults who presented with blunt neck trauma.

Teaching Point

Polytrauma Patients with Obtundation

The American College of Radiology currently recommends cervical spine CT for patients with distracting injuries or other positive findings (9). On the basis of recent evidence, the suggestion is that for alert blunt trauma patients with major distracting injuries who are asymptomatic for cervical spine injury, imaging may not be needed to exclude cervical injuries. Rose et al (10) found an overall sensitivity of 99% for findings from clinical examination alone in a prospective cohort of 761 patients who suffered blunt trauma and had a Glasgow Coma Scale score greater than 14.

As many as one-third of polytrauma patients have a closed head injury, a finding that increases the risk of cervical spine injury by 8.5% (11,12). Others require analgesia or sedation, which can mask evidence of neurologic compromise (12). Missed or delayed diagnoses in these patients produce 10 times the rate of secondary neurologic injury (12,13), whereas early discontinuation of cervical spine precautions is associated with fewer complications, fewer days of mechanical ventilation, and shorter stays in the intensive care unit (14).

The rate of missed injury with conventional radiography is high; in a retrospective evaluation of 800 patients with polytrauma, Nuñez et al (15) found that CT could be used to identify fractures with a sensitivity of 98.5%, compared with a sensitivity of 43% for radiography. Concerns have lingered with regard to the cost and increased radiation of CT because there is a difference of nearly two orders of magnitude in the effective dose between the two modalities. Recently, Theocharopoulos et al (16) tested a risk-benefit decision analysis model comparing radiography and CT in a hypothetical cohort of 1 million patients and found that the higher diagnostic accuracy of CT counterbalanced the increased estimated lifetime cancer risk and monetary cost by substantial margins in both low- and high-risk patients of all ages. These findings support the American College of Radiology's recommendation of screening CT as the standard of care for initial screening of polytrauma patients with obtundation (9).

Controversial Role of MR Imaging for Clearance in Patients with Obtundation

The relative benefit of MR imaging in the clearance of the cervical spine in patients with obtundation who have negative findings at screening cervical spine CT remains a contentious issue. MR imaging has superior sensitivity, compared with that of CT, for evaluating disk and ligament injury but also has a high false-positive rate (17–19). Isolated signal abnormalities without bone injury or abnormal alignment are common but of uncertain importance, sometimes prompting unnecessary spinal immobilization (17). Because of the high sensitivity, several societies recommend MR imaging as the modality of choice in patients expected to be unexaminable for longer than 24–48 hours (9,20).

In 2005, Hogan et al (21) retrospectively evaluated 366 obtunded or "unreliable" patients who had exclusion of unstable cervical spine injury with both multidetector CT and MR imaging, and these investigators found that CT had a negative predictive value of 98.9% for ligament injury and 100% for unstable cervical spine injury. None of the MR imaging findings required treatment as unstable injuries. The preponderance of available evidence, including evidence from several large studies and a meta-analysis of 17 studies with 14,327 patients (19), favors early discontinuation of cervical spine precautions on the basis of CT alone in polytrauma patients with obtundation because few patients with positive MR imaging findings but negative CT findings require a change in management or develop evidence of delayed instability (22,23). Studies with findings that support MR imaging for cervical spine clearance when CT findings are negative are small, few in number, and prone to verification bias because prolonged collar immobilization is often used as an end point (24,25).

Technique

At the R Adams Cowley Shock Trauma Center (Baltimore, Md) and the Ryder Trauma Center (Miami, Fla), a dedicated neck CT angiography protocol is used for isolated neck trauma. Also, continuous-pass whole-body CT angiography is performed in the case of generalized polytrauma.

CT angiography is performed because *(a)* vascular injury can result from traction of vessels against adjacent, sometimes fractured or dislocated bone structures during extreme hyperflexion or extension (26); *(b)* blunt cerebrovascular injury is frequently masked in patients with obtundation (27); and *(c)* injuries may be clinically silent for long periods, later manifesting with ischemia, with a mortality as high as 38% (28). Although digital subtraction angiography remains the reference standard, routine screening CT angiography has been shown to improve morbidity and mortality related to blunt cerebrovascular injury and appears to be cost-effective (28,29).

Although results are conflicting with regard to the diagnostic performance of CT angiography and its suitability as a first-line screening test (30,31), many centers now use CT angiography as the initial screening examination because of practical considerations; CT angiography is considerably less labor-intensive and time-consuming than digital subtraction angiography, is less expensive, and has a much lower risk profile (30), allowing more-liberalized screening protocols that incorporate a greater number of risk factors as indications. These risk factors are listed in Table 2 (26,27). Common findings and grading scales used in the diagnosis of blunt cerebrovascular injury are beyond the scope of this article, and the reader is referred to the 2008 article by Sliker (26) for a comprehensive discussion of this topic.

Table 2: Risk Factors for Blunt Cerebrovascular Injury

Le Fort II or III facial fractures
Skull base fracture extending to petrous internal carotid artery canal
Fractures of C1–C3
Fracture line reaching a transverse foramen
Facet subluxation or dislocation
Scalp degloving injury
Severe mandibular fractures
Closed head injury
Major chest trauma

Dedicated neck CT angiography is performed with the patient's arms down as a single acquisition from the circle of Willis to the aortic arch, with the use of bolus tracking. Whole-body scans are generally performed with the patient's arms elevated alongside the head and neck. Scanning is extended to the pubic symphysis or can include

Table 3: Representative Protocols for CT Angiography

Variable	Whole-Body CT Angiography	Neck CT Angiography
Head CT	Nonenhanced	Nonenhanced
Arm position	Arms raised	Arms down
Intravenous contrast material injection	100 mL	100 mL
Contrast-enhanced imaging	20-second delay (25-sec delay if >55 y)	Bolus tracking
Acquisition	Single acquisition, circle of Willis to symphysis pubis	Circle of Willis to aortic arch
Scan parameters		
Peak voltage (kVp)	120	120
Pitch	0.7	0.7
Revolution time (sec)	0.5	0.5
Collimation (mm)	0.6	0.6
Reconstruction interval (mm)		
Three-dimensional post-processing	1.5	1.5
Primary interpretation	3.0	3.0

the lower extremities when complex extremity fractures are suspected. A fixed delay of 17–20 seconds is used for the whole-body protocol for patients younger than 55 years old, and an additional 5 seconds of delay are added in patients older than 55 years because peak enhancement is slightly delayed in this population (32). Representative protocols for 64-section dedicated neck and whole-body trauma CT angiography are shown in Table 3.

Sliker et al (33) have shown previously that neck CT angiography integrated into the whole-body scan has equivalent diagnostic performance to dedicated CT angiography of the neck despite *(a)* increased quantum mottle from arm elevation and *(b)* the use of a fixed delay. Coronal and sagittal multiplanar reformatted images are routinely generated by the technologist for both dedicated neck and whole-body scans, and thin-slab maximum intensity projection (MIP) images are generated for neck CT angiography. Additional postprocessing is performed by the interpreting radiologist as needed, using thin-client software (TeraRecon, Foster City, Calif) that is available on all workstations.

Select patients with low-energy trauma, such as elderly individuals being evaluated for injuries to the head or face after a fall from standing, sometimes undergo nonenhanced cervical spine CT in conjunction with head and facial CT.

Primary image review should always be performed by using a combination of axial and standard coronal and sagittal reformatted images, and three-dimensional rendering should be used on an as-needed basis for problem solving and to facilitate communication with the surgical team. Evaluation in nonstandard planes by using postprocessing software improves the detection of fractures and aids in inspection of anatomic relationships of the craniocervical junction and subaxial cervical spine (34–36). Additionally, three-dimensional images play a role in characterizing dislocations and subluxations with rotatory components (36) and have great value as an educational tool.

Injuries of the Craniocervical Junction

Craniocervical Dissociation

Craniocervical dissociation is an umbrella term that describes both *(a)* complete dislocations, which are common in fatal motor vehicle trauma, and *(b)* subluxation or distraction injuries, which may be subtle and potentially survivable (34,37). Traumatic atlanto-occipital dissociation is more common and more survivable in skeletally immature pediatric trauma patients; in a recent series, adults represented 50% of the presenting patients but only six of the 22 patients surviving the perioperative period (38). By definition, atlanto-occipital dissociation is an unstable injury with severe ligamentous disruption and is usually accompanied by severe neurologic deficit (39). Associated closed head injuries and upper cervical spine injuries are the main predictors of outcome (38).

Early detection and treatment are essential in patients with craniocervical distraction; however, the diagnosis is often missed prospectively, regardless of experience level, and is easy to overlook at whole-body CT (40,41). Findings may be

Table 4: Normal Measurements in the Craniocervical Junction

Interval	Ligaments Injured	Radiography Cutoff/Reference	Multidetector CT Cutoff/Reference
Basion-to-dens interval	Alar ligaments, tectorial membrane	12 mm/Harris et al (44)	8.5–9.5 mm/Rojas et al (37), Chang et al (35)
Basion–axial line interval	Alar ligaments, tectorial membrane	>12 mm anterior or 4 mm posterior to the posterior axillary line/ Harris et al (44)	Difficult to reproduce/Rojas et al (37)
Atlantodental interval	Transverse ligament, atlanto-occipital and C1-C2 capsules, tectorial membrane, alar ligaments	3 mm (men), 2.5 mm (women)/Hinck and Hopkins (45)	2 mm/Rojas et al (37)
Atlanto-occipital interval	Atlanto-occipital joint capsules, alar ligaments, tectorial membrane	No data in adults	4.0 mm (summed)/Chang et al (35); 2.5 mm (single atlanto-occipital interval)/Rojas et al (37)
Atlantoaxial interval	C1-C2 joint capsules, alar ligaments, tectorial membrane	No data in adults	Midsagittal, 2.6–4.0 mm/ Gonzalez et al (46), Chaput et al (41); lateral margins, 1.2 mm/Radcliff et al (47); posterior and anterior margins, 1 mm/Gonzalez et al (46)
Powers ratio	Transverse ligament, atlanto-occipital joint capsules, tectorial membrane, alar ligament	Anteriorly displaced atlanto-occipital distraction indicated by Powers ratio >1/ Powers et al (42)	Anteriorly displaced atlanto-occipital distraction indicated by Powers ratio >1/Dziurzynski et al (43)

subtle, and qualitative evaluation is often not sufficient. In the past several years, a number of craniocervical measurements that were established by using conventional radiography have been re-assessed with CT (Table 4) (35,37,41–47). Normal intervals for the most commonly used measurements are shown in Figure 1, and examples of craniocervical distraction injuries with abnormal relationships are shown in Figure 2.

The Powers ratio (ratio of the distance from the posterior margin of the foramen magnum to the anterior arch of the atlas divided by the distance from the tip of the basion to the posterior arch of C1) (42) has also been assessed with CT in a small series (43) and was found to have a sensitivity of 74% when a value of 1.0 was used as the upper limit of normal. The Wackenheim basilar line (drawn along the dorsal margin of the clivus) should normally intercept the tip of the dens. The utility of this line for diagnosing craniocervical distraction is controversial in the trauma setting (48) and has not been well explored by using CT.

At the atlantoaxial articulation, the presence of a cranially divergent predental angle ("V sign") is suggestive of transverse ligament injury and also increases the likelihood of atlanto-occipital distraction (35). Isolated distraction of the C1-C2 lateral masses is uncommon and typically occurs without cruciate ligament injury or neurologic sequelae. One group of investigators has classified craniocervical distractions into type I (isolated atlantoaxial injuries) and type II (combined atlanto-occipital and atlantoaxial injuries) (49).

Abnormal values tend to be sensitive but not specific. Although normal intervals virtually rule out craniocervical distraction, values greater than established upper limits can be normal in some patients but abnormal in others. In a recent series of 18 patients with atlanto-occipital dissociation, evidence of atlanto-occipital capsular injury on MR images was always associated with some degree of articular displacement in the abnormal range (49).

Occipital Condyle Injuries

Occipital condyle fractures have a 3% incidence in patients with severe blunt cervical trauma, occur in as many as 16% of craniocervical injuries, and should be considered markers of a high-energy mechanism of injury (50,51). Most occipital condyle fractures are associated with closed head injury, although a substantial proportion of patients with such fractures have

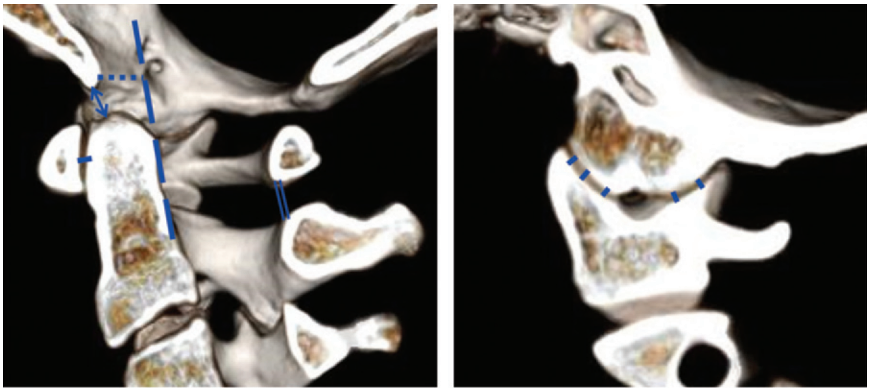

a. b.

Figure 1. Normal intervals of the craniocervical junction. **(a)** Midsagittal half-space volume-rendered CT image shows the atlantodental interval (solid line), the basion-dens interval (double-headed arrow), the posterior axial line (dashed line), the basion-to–posterior axial line interval (dotted line), and the C1–C2 spinolaminar distance (parallel lines). **(b)** Volume-rendered CT image shows the normal relationship of an occipital condyle and the lateral mass of C1, with close apposition, and the nearly equidistant intervals (solid lines) along all points in the midsagittal plane of the joint.

normal Glasgow Coma Scale scores (52). Associated injuries that may be seen at CT include facial fractures, vertebral and carotid artery injuries, and fractures anywhere along the cervical spinal column (52).

Classification of Occipital Condyle Fractures

Anderson and Montesano (53) introduced the most widely used radiologic classification system for occipital condyle fractures, describing three different patterns of injury: *(a)* comminution-impaction injury resulting from axial loading, with minimal or no fracture displacement (type I) (Fig 3a); *(b)* skull base fracture extending through the occipital condyle, resulting from a direct blow to the skull (type II) (Fig 3b); and *(c)* avulsion fracture resulting from tension on the alar ligament from forced rotation and lateral bending (type III) (Fig 3c) (Table 5) (53–58).

Type I and II injuries are thought to be stable, with preservation of the alar ligaments. Type III fractures, in which the alar ligaments are disrupted or functionally incompetent from bone avulsion, are unstable and may cause neurologic injury from excessive motion or displaced condylar fragments (51,53).

Fractures may be unilateral with minimal distraction, may be bilateral, or may extend in a ringlike configuration along the anterior foramen magnum, with bilaterality increasing the likelihood of instability (36,50). Approximately 75% of occipital condyle fractures are type III injuries (51). Differentiating between type I occipital condyle fractures with minimal displacement and type III occipital condyle fractures may be difficult at multidetector CT. An MR imaging–based classification scheme has been introduced by Tuli et al (59) to determine stability on the basis of direct depiction of ligament integrity.

Fractures of the Atlas

Atlas fractures account for 25% of craniocervical injuries. As many as 44% of atlas fractures have associated fractures of the axis. Jefferson introduced the first classification system for atlas fractures, which is still in use with some modifications (54,60). Fractures of the posterior arches alone are type I (Fig 4a). Isolated fractures of the anterior arch are type II. Bilateral posterior arch fractures with unilateral or bilateral anterior arch fracture are type III (classic Jefferson burst) (Fig 4b). Fractures of the lateral mass are type IV. Transversely oriented anterior arch fractures resulting from avulsion of the longus colli or atlantoaxial ligament are type V (60).

Bilateral fractures of the posterior arches and burst fractures are the most common patterns. Isolated anterior arch fractures are relatively rare (61,62).

Fractures of the atlas are usually mechanically stable and rarely result in neurologic injury. For atlas fractures, associated cervical spine fractures and the integrity of the transverse ligament are the main determinants of the need for surgical intervention (60).

Jefferson Fractures

Burst fractures of the atlas are thought to result from axial loading. Fractures through the anterior

Figure 2. Widened intervals in craniocervical distraction injuries in four patients. **(a)** Half-space slab volume-rendered CT image of a patient with atlanto-occipital dissociation after an MVC shows the "V sign" of cranially divergent predental lines (solid lines), a widened basion-dens interval (double-headed arrow), the posterior axial line (dashed line), a widened basion-to–posterior axial line interval (dotted line), and a widened C1–C2 spinolaminar interval (parallel lines). **(b)** Volume-rendered CT image of a 45-year-old patient after an MVC shows a widened atlantodental interval (solid line) secondary to a transverse ligament injury. **(c)** Coronal volume-rendered CT image of a 26-year-old man with craniocervical distraction after a motorcycle collision was obtained with a "virtual radiograph" template and shows bilateral widening of the atlanto-occipital joints *(AO)* and the atlantoaxial joints *(AA)*. **(d)** Volume-rendered CT image of a 23-year-old man with craniocervical distraction after a motorcycle collision shows the occipital condyles *(OC)* dissociated from the lateral masses of the atlas and shifted anteriorly. **(e)** Midsagittal half-space slab volume-rendered CT image of a 23-year-old man (same patient as in **d**) shows a marked widening (solid lines) of the atlanto-occipital articulation, with anterior translation of the condyles and skull base.

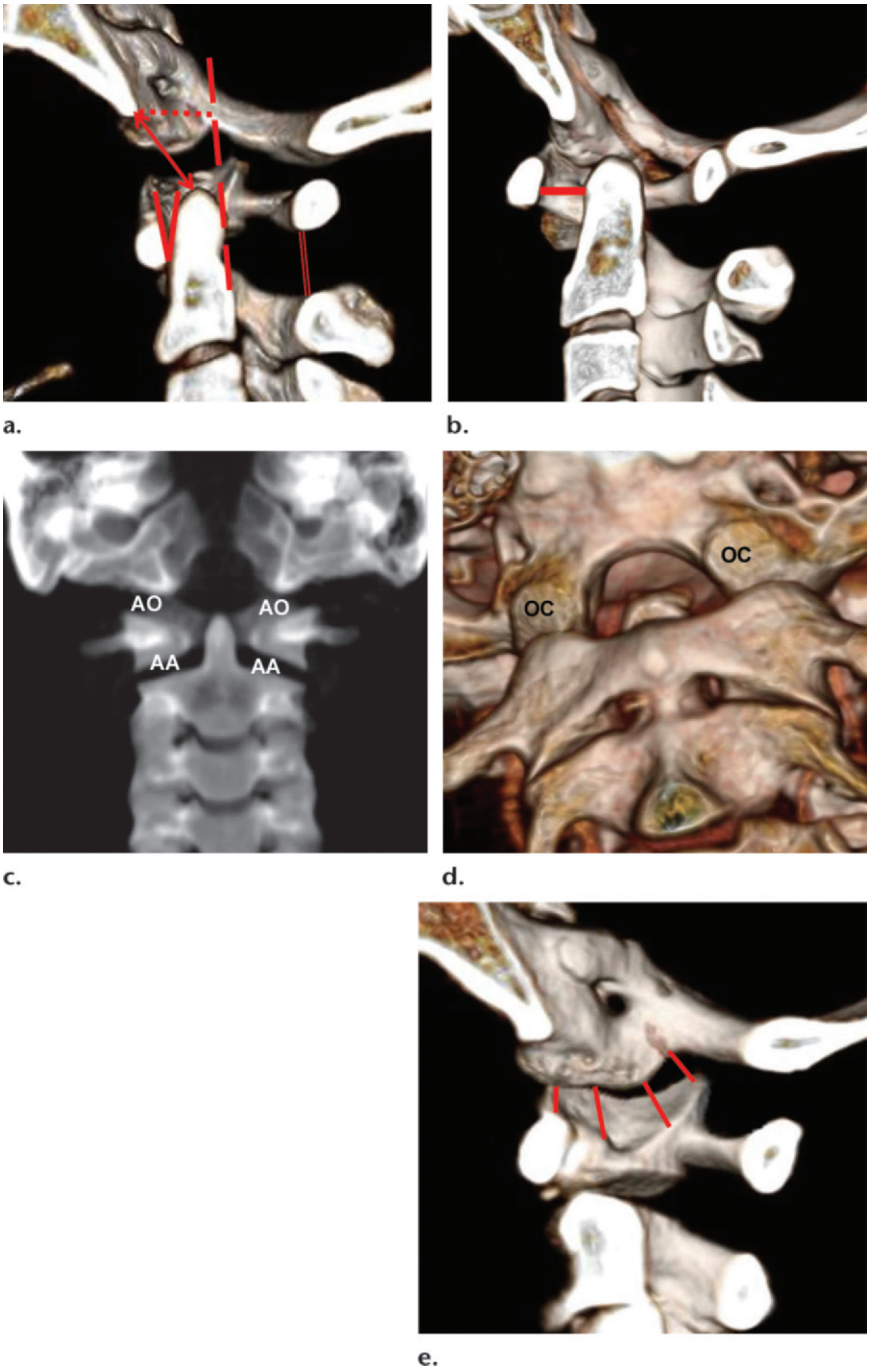

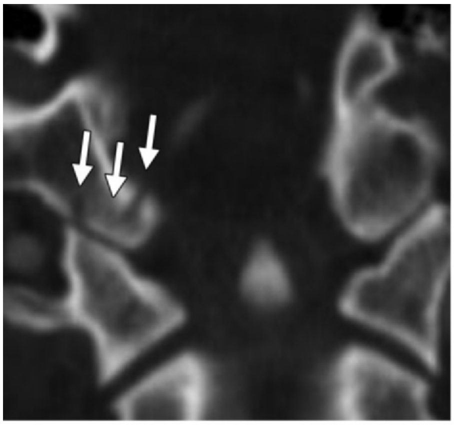

a.

Figure 3. Occipital condyle fractures in three patients. **(a)** Coronal multiplanar reformatted CT image of a 24-year-old man after a motorcycle collision shows a right type I condylar fracture (arrows) resulting from impaction of the condyle against the right lateral mass of C1. **(b)** Off-axial MIP image of a 52-year-old man after an MVC shows a type II right occipital condyle fracture associated with a skull base fracture (arrows). **(c)** Coronal MIP image of an 18-year-old man with severe polytrauma after an MVC shows an avulsion fragment off the right occipital condyle (type III occipital condyle fracture).

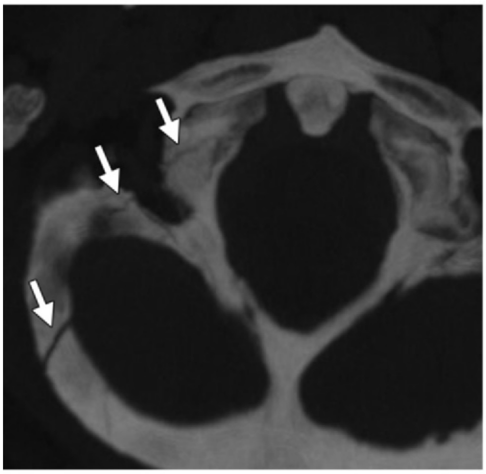

b.

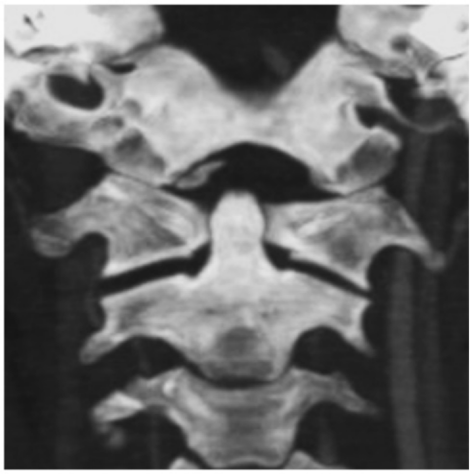

c.

or posterior arches may be single along the midline, or bilateral with a number of permutations. An atypical Jefferson burst with unilateral anterior and posterior arch fractures is shown in Figure 4c. The fracture pattern results in outward displacement of the lateral masses, a finding that indicates possible injury to the transverse ligament.

To prevent atlantoaxial dissociation, Jefferson fractures may require surgical stabilization if the transverse ligament is compromised or the anterior arch is appreciably displaced. At radiography, a combined sum of lateral mass displacement measuring 6.9 mm was identified as a predictor of transverse ligament disruption ("rule of Spence") (63). Subsequently, Dickman et al (64) showed that applying the rule of Spence would have missed 61% of fractures. Absence of magnification at cross-sectional imaging may account for this poor performance (65), but a useful smaller cutoff value has not been established for CT, to our knowledge. Dickman et al (64) provided a new CT and MR imaging–based classification; disruptions of the ligament substance are type I injuries. Avulsions of the tubercle at the insertion on the lateral mass are type II. Type II injuries are physiologically incompetent even though the ligament is not torn. A total of 74% of type II injuries healed with rigid cervical orthosis, whereas none of 15 patients with type I injuries healed with nonsurgical treatment (64).

Fractures of the Axis

Approximately 17%–20% of cervical spine fractures involve the axis (66). Odontoid fractures, hangman fractures, and fractures of the axis body account for the three main types of injury patterns (67).

Odontoid Fractures.—Odontoid fractures represent the most common fracture of the axis, accounting for approximately 59% of cases in a series of 340 axis fractures (66). The incidence of odontoid fractures appears to be higher in elderly patients and may be related to the increased transmission of forces to the dens in stiff spondylotic spines (68).

A three-part classification system for odontoid fractures proposed by Anderson and D'Alonzo (55) in 1974 has gained wide acceptance. Type I odontoid fractures are obliquely oriented fractures through the tip of the odontoid, likely representing avulsions of the alar ligament (Fig 5a).

Table 5: Craniocervical Injury Classification Systems

Types of Craniocervical Injury (Classification System Reference)	Stability
Occipital condyle fractures (Anderson and Montesano [53])	
Type I: axial loading with minimal or no fracture displacement	Stable
Type II: skull base fracture extending through the condyle	Stable
Type III: alar ligament avulsion fracture	Unstable
Atlas fractures (Jefferson, as modified by Gehweiler et al [54])	
Type I: posterior arches	Stable
Type II: anterior arch	Stable
Type III: bilateral posterior arch with bilateral or single unilateral anterior arch ("Jefferson burst")	Depends on integrity of transverse ligament
Type IV: lateral mass	Stable
Type V: transversely oriented anterior arch fractures (avulsion of longus colli or atlantoaxial ligament)	Stable
Odontoid fractures (Anderson and D'Alonzo [55])	
Type I: oblique fracture through the tip of the odontoid, result of alar ligament avulsion	Stable
Type II: dens-body junction	Unstable*
Type III: cancellous portion of the axis body	Heals well with immobilization but can cause canal compromise
Hangman fractures (Effendi et al [56], modified by Levine and Edwards [57])	
Type I: hairline fractures, <2-mm translation	Stable
Type II: angulation > 11°, >2-mm translation	Variable, external immobilization often used
Type IIa: severe angulation without translation, intact anterior longitudinal ligament	Angulation can worsen with initial traction
Type III: bilateral facet dislocation	Unstable
Atlantoaxial rotatory subluxation and fixation (Fielding and Hawkins [58])	
Type I: rotatory fixation in normal physiologic range (<48°–52° left or right), dens acts as a pivot, intact alar and transverse ligaments	Need for surgery depends on degree of rotation, prognosis improves with early reduction
Type II: transverse ligament injured, center of rotation shifts to lateral mass, anterior displacement of the atlas < 5 mm	Unstable
Type III: transverse and alar ligaments both deficient, similar to type II but anterior displacement of the atlas > 5 mm	Unstable
Type IV: deficient odontoid, with posterior displacement of the atlas	Unstable

*The risk factors for nonfusion of type II odontoid fractures are *(a)* age older than 50 years, *(b)* 6 mm or more of dens displacement, and *(c)* comminution and splinter fragments at the fracture site.

These odontoid fractures are the least common, accounting for 1%–3% of cases (55,66,67), with a bone fusion rate approaching 100% with the use of collar or halo immobilization (69,70).

Type II odontoid fractures occur at the junction of the dens and body and are the most common odontoid fractures, representing 54%–60% of cases (Fig 5b). In a study of 107 axis fractures, Hadley et al (71) found that nonunion occurred in approximately 26% of the patients with type II fractures who were treated nonsurgically. When there was a 6-mm or greater displacement of the dens, the incidence of nonunion in type II odontoid fractures increased to 67% (71). In several studies, investigators have documented a correlation between increasing fracture gap and nonunion (72,73). Age older than 50 years is another significant risk factor (P = .002) (74). Type II odontoid fractures with comminution and splinter fragments at the fracture site were described as highly unstable, with a greatly increased rate of nonfusion, by Hadley et al (75) in 1988 and were subcategorized as type IIa (Fig 5c). These injuries are rare, but subtle comminution is appreciated with increased frequency at multidetector CT (76). The clinical importance of small splinter fragments with regard to stability remains uncertain. The risk factors for nonfusion of type II odontoid fractures

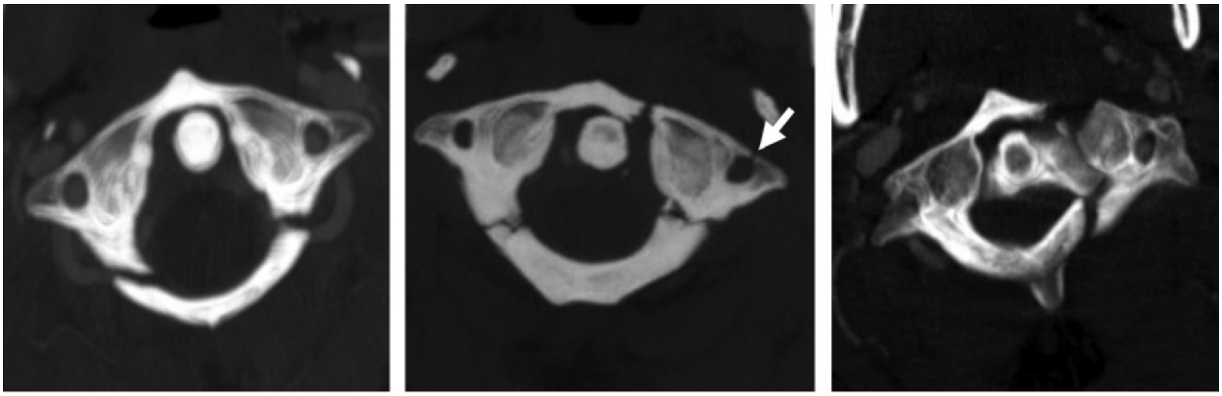

a. b. c.

Figure 4. Fractures of the atlas in three patients. **(a)** Off-axial MIP image of a 27-year-old woman after an MVC shows bilateral posterior arch fractures. Head rotation within the physiologic range results in asymmetry of the lateral atlantodental intervals. **(b)** Off-axial MIP image of a 49-year-old woman after an MVC shows a three-part Jefferson fracture of the atlas. A congenital cleft (arrow) is incidentally depicted anteriorly at the foramen transversarium. The cleft is distinguished from a fracture by its smooth sclerotic appearance and because ring fractures should occur in at least two parts. The patient also had burst fractures at T5 and T6 related to the axial loading mechanism (not shown). **(c)** Off-axial MIP image of a 50-year-old female pedestrian who was struck by a motor vehicle shows unilateral fractures of the left anterior and posterior arches, with separation of the lateral mass.

are *(a)* age older than 50 years, *(b)* 6 mm or more of dens displacement, and *(c)* comminution and splinter fragments at the fracture site.

Type III odontoid fractures make up 39%–42% of cases (67). In type III fractures, the fracture line extends through the cancellous portion of the C2 body (Fig 5d, 5e). These fractures are potentially mechanically unstable because the atlas and dens can move together as a unit (77), but type III odontoid fractures heal with immobilization in 88% of cases, and surgical fusion is often not necessary (69,70).

Hangman Fractures.—Bilateral pars interarticularis fractures associated with judicial hanging were first described in 1913 by Wood-Jones (78). “Hangman’s fracture” as an eponym for traumatic spondylolysis of the axis was first used by Schneider et al (79) in 1965 as a catchall for these injuries in victims of MVCs and other sudden deceleration accidents (67). In spite of the name, these fractures can occur as the result of either compressive hyperextension or distractive hyperflexion and can involve any part of the axis ring, including laminae, pedicles, or part of the posterior wall of the axis body (56,80).

Hangman fractures (now sometimes referred to as “hanged man fractures”) account for 22% of axis fractures and 4% of cervical fractures overall. Both hangman fractures and Jefferson fractures decompress the already spacious canal at this level. Hangman fractures are associated with neurologic sequelae in only 26% of cases (81). Most hangman fractures are treated successfully with immobilization (56,57). Associated atlas fractures are seen in 6%–26% of cases (67), and fractures of other cervical vertebrae occur in 8%–32% of cases (66,80).

Classification of Hangman Fractures.—In the most commonly used system for classification of hangman fractures, which was initially proposed by Effendi et al (56) and was modified by Levine and Edwards (57), type I hangman fractures are minimally displaced, are associated with less than 2-mm translation, and have no associated angulation or posterior intervertebral disk space widening (Fig 6a, 6b). Type I injuries are considered stable and are treated only with cervical orthosis. Levine and Edwards (57) attributed type I injuries to a hyperextension–axial loading mechanism and noted an association with Jefferson, odontoid, and posterior arch C1 fractures.

Type II hangman fractures are characterized by anterior angulation (>11°) and anterior translation (Fig 6c), with fractures resulting from distractive flexion or compressive hyperextension (56,57). These injuries are treated with halo traction and immobilization. Associated anterosuperior C3 wedge compression deformities or C2 endplate avulsion fractures may result. An atypical type II hangman fracture involving part of the wall of the axis body was seen in a patient (Fig 6d, 6e). Levine and Edwards (57) classified hangman fracture injuries with minimal or no translation but severe angulation as type IIa, in which the anterior longitudinal ligament remains intact (Fig 6f). Type IIa injuries may become more angulated with traction and require reduction with gentle extension before immobilization with a halo vest.

Figure 5. Odontoid fractures in four patients. **(a)** Coronal multiplanar reformatted CT image of a 51-year-old man after a motorcycle collision shows an oblique fracture of the odontoid tip (type I odontoid fracture). **(b)** Coronal half-space volume-rendered CT image of a 24-year-old patient after a rollover MVC shows a type II odontoid fracture. **(c)** Sagittal MIP image of an 86-year-old patient after a fall from standing shows a type IIa odontoid fracture with posterior displacement, posterior angulation, and comminution. **(d)** Coronal multiplanar reformatted CT image of a 78-year-old patient involved in an MVC shows a type III dens fracture (arrows). **(e)** Lordotic volume-rendered CT image of a 78-year-old patient (same patient as in **d**) shows anterior displacement of the fractured dens *(D)* and the involved superior portion of the C2 body. *A* = atlas, *B* = fragment of the C2 body, *U* = undersurface of the C2 body fragment.

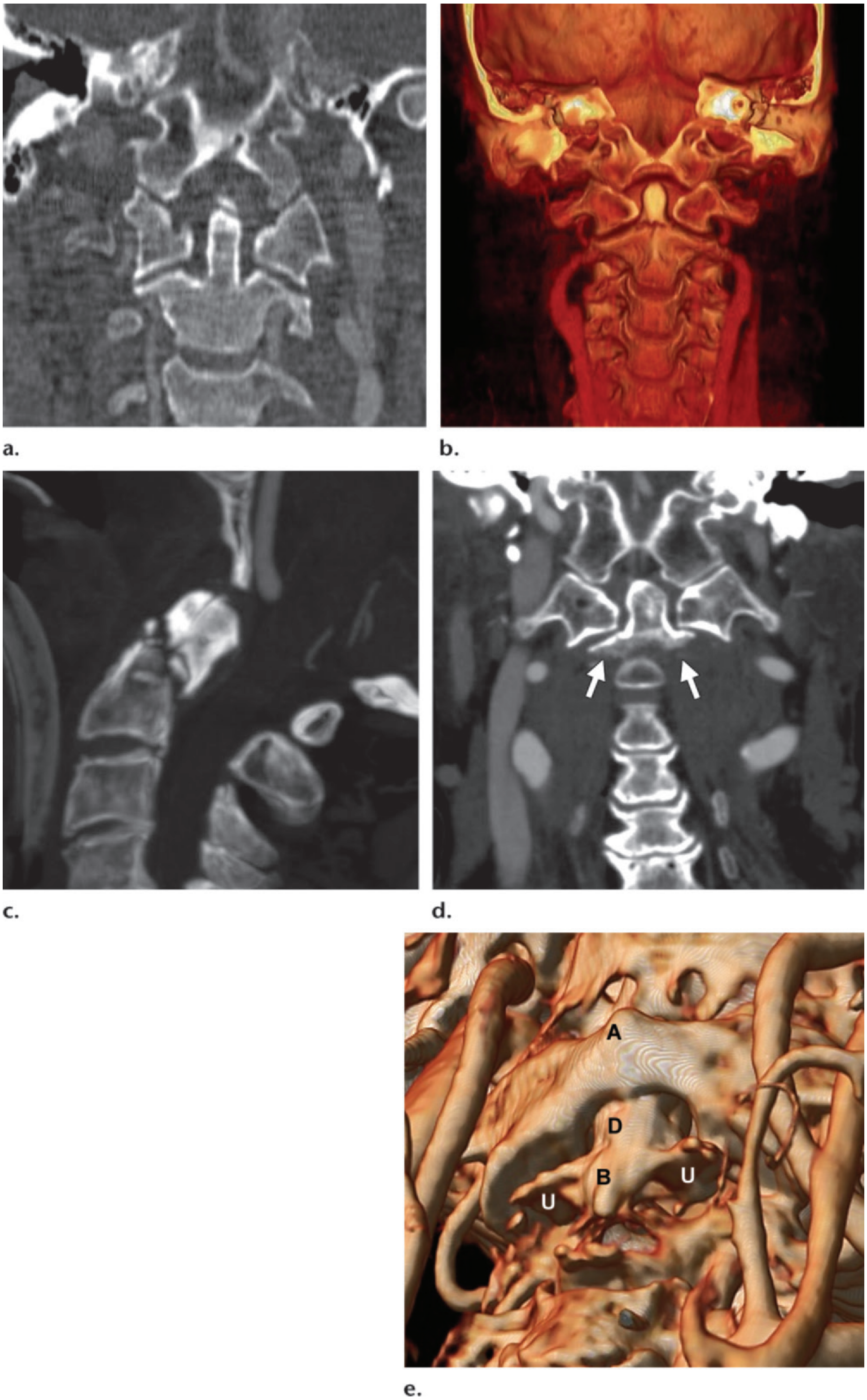

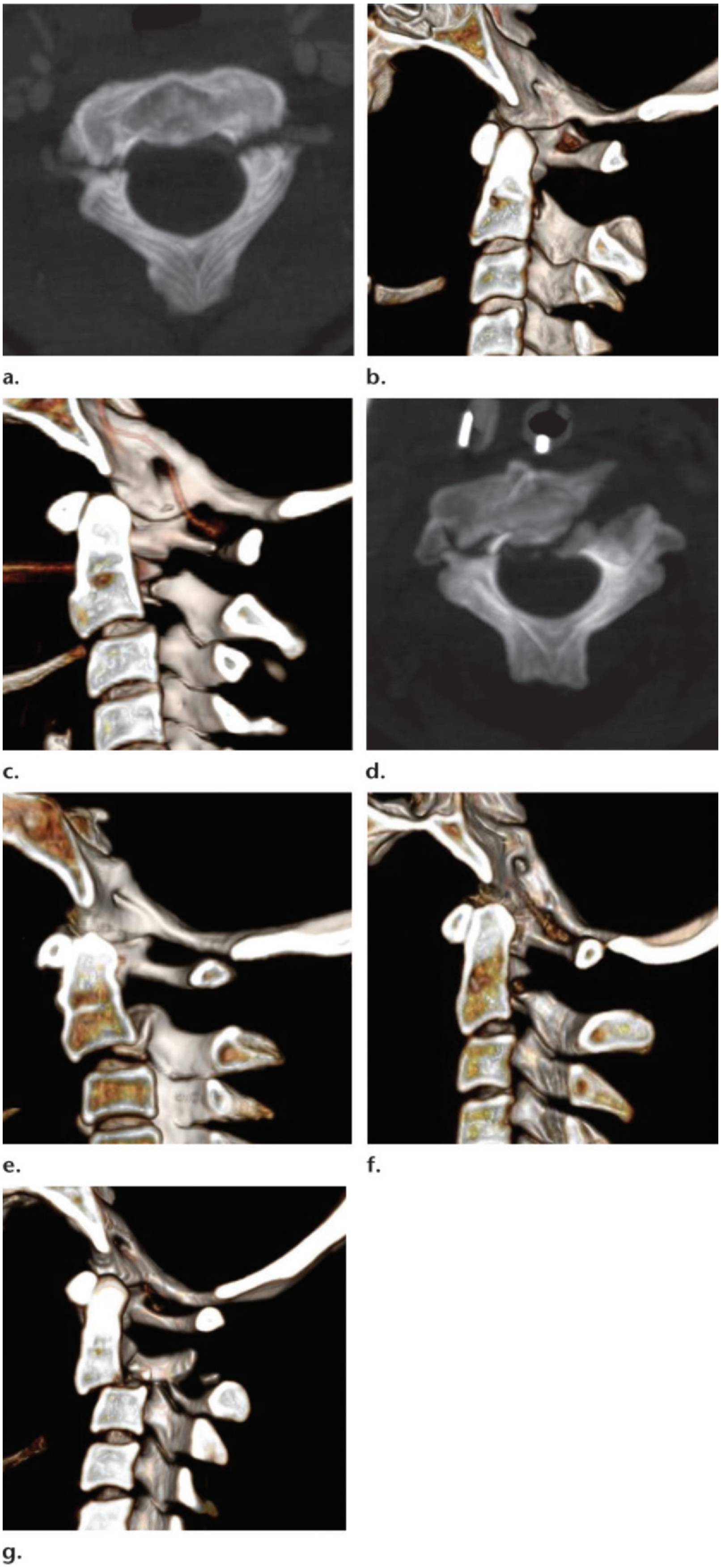

Figure 6. Hangman fractures in five patients. **(a)** Off-axial MIP image of an 18-year-old patient after a fall from an all-terrain vehicle shows a type I hangman fracture with bilateral fractures of the pars interarticularis. **(b)** Sagittal half-space slab volume-rendered CT image of an 18-year-old patient (same patient as in **a**) shows no translation or angulation of C2. **(c)** Sagittal half-space slab volume-rendered CT image of a 27-year-old woman with a type II hangman fracture after an MVC shows anterior translation and angulation of C2. The patient also had bilateral posterior arch fractures from hyperextension. **(d)** Off-axial MIP image of a 62-year-old woman with an atypical type II hangman fracture after an MVC shows a pars fracture on the right and an oblique fracture through the posterolateral vertebral body. **(e)** Sagittal half-space slab volume-rendered CT image of a 62-year-old woman (same patient as in **d**) shows anterior translation and angulation of C2 and a fracture involving the left vertebral body. **(f)** Sagittal half-space slab volume-rendered CT image of a 26-year-old woman with a type IIa hangman fracture after an MVC shows a pars interarticularis fracture with anterior angulation of the body of C2 but no anterior translation. No disruption of the anterior longitudinal ligament was depicted on MR images (not shown). **(g)** Sagittal half-space slab volume-rendered CT image of a 30-year-old woman with a type III hangman fracture after an MVC shows marked anterior translation of C2 with facet fracture-dislocation.

Type III injuries are the least common, representing 7%–10% of hangman fractures, and result from severe distractive flexion with associated bilateral facet dislocation or fracture-dislocation (Fig 6g). These injuries are analogous to distractive injuries in the subaxial spine and require surgical stabilization (57).

Axis Body Fractures.—Fractures of the axis body are the most common subtype of a group of fractures first referred to by Hadley et al (71) as "miscellaneous non-odontoid non-hangman fractures of the axis," which represent the remaining 19%–32% of axis fractures (82) and include isolated lateral mass fractures (Fig 7), pedicle fractures, and transverse process fractures. Axis body fractures have a variety of morphologic structures and orientations and also include burst injuries. These injuries are often inherently stable and can usually be treated nonsurgically.

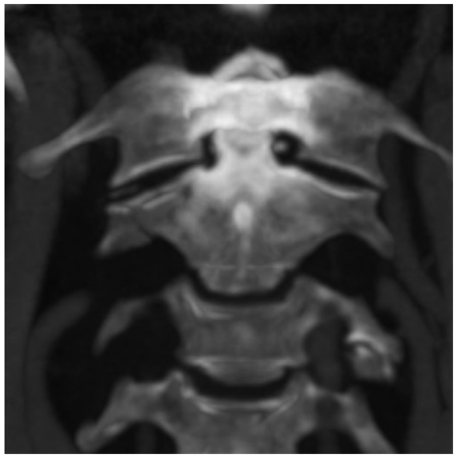

Figure 7. Nonodontoid nonhangman fracture. Coronal MIP image of a 73-year-old man after an MVC shows a nonodontoid nonhangman fracture involving the right lateral mass of C2.

Atlantoaxial Rotatory Subluxation and Fixation

Traumatic rotatory subluxation and fixation are well documented in children but are rare in adults, with few reported cases (83). In normal individuals, rotation at the atlantoaxial joint can be as high as 48°–52° to one side (84). Bifacet dislocation is expected to occur at an average of 63°–64°. Higher degrees of rotatory subluxation have a greater propensity to develop into rotatory fixation and have a greater need for surgical reduction. Early diagnosis may prevent permanent deformity (85). The exact cause of fixation is not known but is suspected to be capsular and synovial swelling or a tear in the early stage after injury, ultimately resulting in contractures.

Classification of Atlantoaxial Rotatory Fixation

Fielding and Hawkins (58) have described a number of configurations of atlantoaxial rotatory fixation. Type I atlantoaxial rotatory fixation occurs within the normal physiologic range, with intact alar and transverse ligaments. The dens acts as the pivot, and there is no anterior displacement of the atlas (58). In type II atlantoaxial rotatory fixation, the transverse ligament is injured. This injury causes the center of rotation to shift to one of the lateral masses. Anterior displacement of the atlas should not exceed 5 mm because of restraint from the alar ligament.

In type III atlantoaxial rotatory fixation, both the transverse and alar ligaments are deficient. The configuration is similar to type II, but anterior displacement of the atlas exceeds 5 mm. Type IV describes the rare circumstance in which a deficient odontoid is present, resulting in posterior displacement of the atlas. The spinal canal may be compromised in types II to IV.

Rotatory subluxation may be associated with a contracted sternocleidomastoid muscle on the ipsilateral side of the head. Diagnosis of fixation is often delayed, and fixation should be suspected when torticollis does not resolve within 5–7 days after the injury. Dynamic CT imaging is an important problem-solving tool in establishing the diagnosis. CT is performed first with the head in the resting position and then with maximal contralateral rotation (58).

Injuries of the Subaxial Cervical Spine

Subaxial injuries account for 65% of cervical spine fractures and 75% of dislocations (3). Several mechanism-based radiographic classifications specific to the subaxial cervical spine have been introduced. In 1982, on the basis of their retrospective experience with 165 patients, Allen, Ferguson, and colleagues (86) proposed that cervical spines with the same posture, force vectors, and magnitude will result in reproducible injury patterns (87), and these investigators devised a new radiography-based scoring system in which cervical spine trauma was categorized into six "phylogenies" (spectra of injury): flexion compression, vertical compression, flexion-distraction, extension compression, extension distraction, and lateral flexion, with a separate severity scale for each mechanism. This system was subsequently modified by Harris et al (88) to include rotational components in lieu of lateral flexion.

The Allen-Ferguson descriptive terms are used pervasively; however, because of its complexity, the scoring system has not been widely adopted. For example, hyperflexion injuries may

Table 6: SLIC Score Determination

SLIC Categories	Score*
Morphology	
No abnormality	0
Compression	1
Burst	2
Distraction	3
Translation or rotation	4
Discoligamentous complex	
Intact	0
Indeterminate	1
Disrupted	2
Neurologic status	
Intact	0
Root injury	1
Complete cord injury	2
Incomplete cord injury	3
Incomplete cord injury with ongoing cord compression	4

*Total SLIC score: ≤3 = nonsurgical, 4 = indeterminate, ≥5 = surgical.

have both compressive and distractive flexion components, requiring two different scores for the same level of injury. Although mechanistic classifications appear intuitive, Vaccaro et al (3) found that the Allen-Ferguson system has poor inter- and intraobserver variability, which they attributed to *(a)* the wide range of fracture patterns that can result from the same force vectors as the cervical spine buckles with stress and *(b)* the outsized role that the recoil position of the cervical spine played in inferring the injury mechanism (87,89).

To our knowledge, only two scoring systems have been developed that specifically incorporate multidetector CT: the cervical spine Subaxial Injury Classification and Scoring (SLIC) system (3) and the cervical spine injury severity score (90). To date, these two systems have received little attention in the radiology literature. Both systems have limitations but nevertheless mark a new era of cross-sectional imaging–based injury grading. Both de-emphasize the use of mechanism and recoil position in grading injuries and rely on direct assessment of bone morphologic structure. These two systems appear to have higher interobserver reliability compared with the Allen-Ferguson and Harris systems (3,91).

Cervical Spine Injury Severity Score

The cervical spine injury severity score is a CT-specific scoring system originally described by Moore et al (92). Four columns are defined: the anterior, the posterior, and two lateral columns. A value of 0–5 points is assigned to each column on the basis of the degree of displacement and indirect evidence of ligamentous instability. Injuries are classified as *(a)* simple if there is bone injury to a single column or *(b)* complex if either more than one column is involved or there is evidence of both ligamentous and bone injury within a single column. The scores are summed to give a cumulative score ranging from 0 to 20. Surgical fixation is indicated when the score is 7 or more. This paradigm does not take into account the neurologic status or MR imaging findings. Because of its relative complexity, this score is unlikely to gain widespread use in clinical practice.

SLIC System

The SLIC system, which was introduced in 2007 by Vaccaro et al (3), follows the general concept and organization of the thoracolumbar injury classification and severity score, which had been previously developed by the same group of investigators (93). The SLIC system serves to provide a unified, more parsimonious, and easily applicable decision tool for evaluating, grading, and communicating injuries for the entire subaxial spine (3,87,94). The SLIC system is made up of three separately graded components, each ostensibly representing major independent predictors of outcome. The three components of SLIC are *(a)* morphologic findings of bone spinal column disruption, *(b)* the integrity of the discoligamentous complex, and *(c)* neurologic status (95). The three scores for these three components are summed to give the SLIC score (total score). Combined scores of 5 or more indicate the need for surgical intervention. Injuries with scores of 3 or less can be managed without surgery, and scores of 4 are indeterminate (Table 6). The SLIC system is quickly becoming widely adopted because of its ease of use and its potential clinical utility in helping distinguish surgical injuries from nonsurgical injuries.

Teaching Point

SLIC Morphology Score

The SLIC morphology score describes the structural integrity and relationships of vertebrae at an injured motion segment, with higher scores corresponding with worse outcomes and an increased need for surgery (3,94). Morphology can be characterized with CT alone, and complete discoligamentous injury can also usually be diagnosed with a high degree of specificity in more-severe cases. The most severe manifestation of an injury determines the SLIC morphology score. For example, if a burst injury has some associated distraction, it is called a distraction injury; if both distraction and translation are present, this injury is classified as a

Figure 8. Compression burst fracture. Sagittal half-space slab volume-rendered CT image of a 23-year-old man after an MVC shows a burst fracture of C7 without associated facet distraction.

translation injury, and so forth. When multiple levels are involved, a separate score is given to each injured level. A score of 1 is assigned for simple compression, a score of 2 for burst, 3 for distraction, and 4 for translation or rotation.

Compression (Score of 1) and Burst (Score of 2).—Compression and burst fractures are characterized by loss of vertebral body height without evidence of distraction or translation, regardless of whether focal kyphosis is present (Fig 8). Visible endplate disruption or a fracture line in the sagittal or coronal plane may be seen (3,87,94). Fragments with a triangular teardrop morphology should still be characterized as compression injury with a score of 1 or 2 if there is no associated posterior element distraction or vertebral body translation. Undisplaced or minimally displaced lateral mass, facet, laminar, or spinous process fractures without distraction are also classified as compression injuries and may occur in isolation or with vertebral body compression or vertebral burst.

Teaching Point

Distraction (Score of 3).—Distractive injuries of the subaxial cervical spine are characterized by dissociation in the vertical axis. Distraction may occur anteriorly as a result of hyperextension or posteriorly from hyperflexion.

Hyperflexion.—Hyperflexion injuries range from facet subluxation, with decreased apposition or diastasis of the articular surfaces (Fig 9a, 9b), to perched facets (3,95) (Fig 9c, 9d). Facets are considered subluxated when there is less than 50% overlap of the articular surfaces or more than 2 mm of diastasis (3). Associated findings include *(a)* posterior disk space widening with angulation greater than 11° and *(b)* focal kyphotic deformity. Important cutoff values for hyperflexion-type distraction injuries and translation are shown in Table 7. When perched facets impact and fracture or dislocate, they become translational injuries (3,95).

Hyperextension.—Extension-type distraction injury is synonymous with the term *hyperextension dislocation* (96) and results from disruption of the anterior longitudinal ligament and intervertebral disk. Elderly or intoxicated patients who have impaired ability to break a fall are prone to this type of injury. Deceleration injury in MVCs is another common cause. Falls from standing can result in hyperextension injuries with severe cord injury in elderly patients with spondylotic and osteoporotic spines. These injuries manifest with "extension teardrop" fracture, an avulsed fragment of the anterior inferior corner of the involved vertebral body, in 65% of cases (96), most commonly at C2. Extension teardrop fracture is characteristically a thin fracture fragment greater in the horizontal than the vertical dimension, is often associated with anterior disk space widening, and is further differentiated from flexion teardrop by location, with the latter usually occurring at C5 and C6. Evidence of posterior distraction should be absent, and other stigmata of hyperextension injury such as facial trauma and compression fractures of the facets, laminae, and spinous processes may be seen (Fig 10).

Translation or Rotation (Score of 4).—Translation or rotation is demonstrated by vertebral offset in the horizontal axis and may occur with or without fracture. A pure translation of one ver-

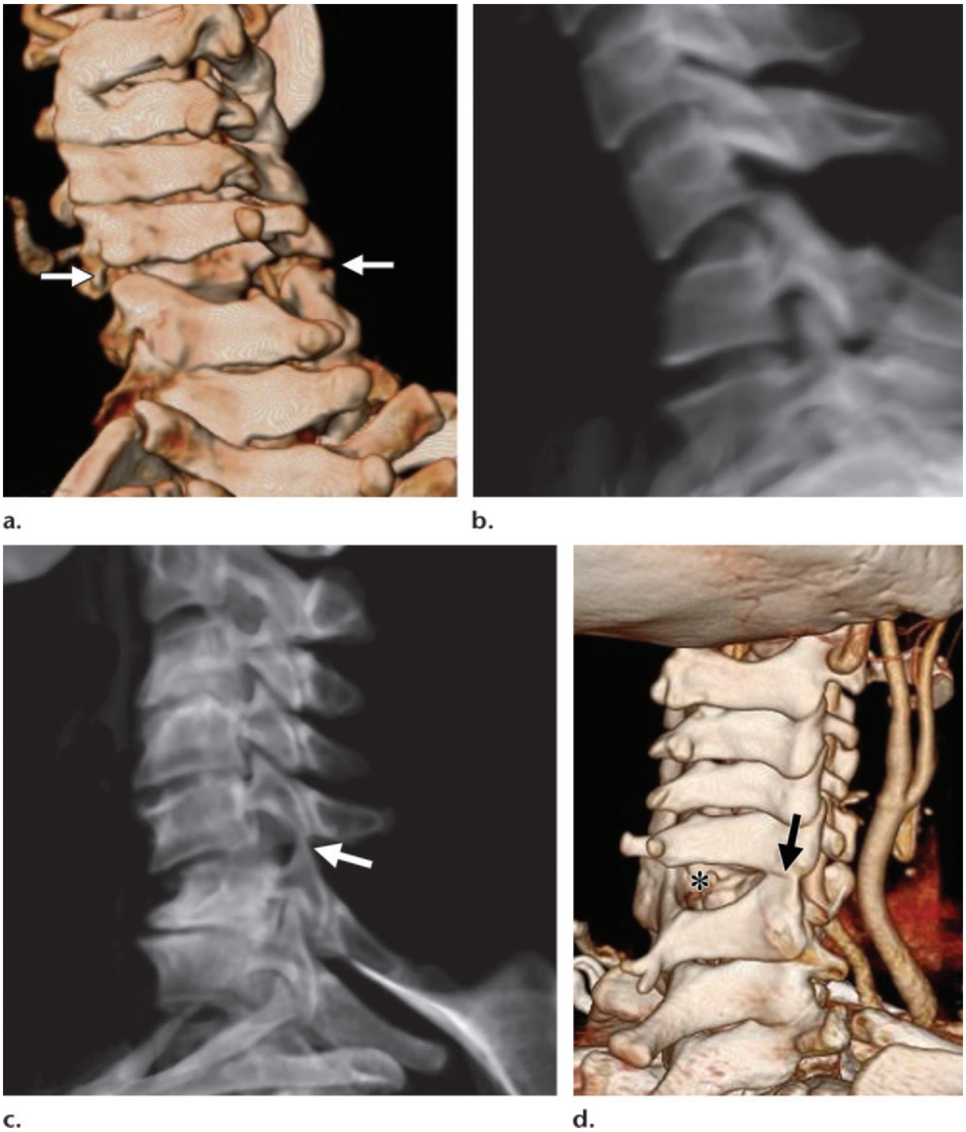

Figure 9. Flexion-distraction injuries in two patients. **(a)** Oblique volume-rendered CT image of a 39-year-old woman after an MVC shows bilateral C5-C6 facet distraction (arrows). **(b)** Sagittal "virtual radiograph" volume-rendered CT image of a 39-year-old woman (same patient as in **a**) shows C5-C6 kyphotic angulation and posterior disk space widening. **(c)** Sagittal "virtual radiograph" volume-rendered CT image of a 43-year-old woman who fell a short distance and landed on her head shows perched facets (arrow) at C5-C6, with focal kyphotic deformity. **(d)** Oblique volume-rendered CT image of a 43-year-old woman (same patient as in **c**) shows interspinous widening (*) associated with the C5-C6 facet perch (arrow).

tebra relative to another may occur when discoligamentous structures are disrupted bilaterally, or rotation may occur when an intact facet serves as a pivot point (87,95).

Translation or rotation injuries can result from unilateral or bilateral facet dislocations or fracture-dislocations (Fig 11a, 11b). Normal spinal alignment is shown for comparison (Fig 11c). A horizontal distance of 3.5 mm between the posterior aspects of the rostral and caudal vertebral body at any given motion segment is used as a cutoff for translational injury (3,94). Traumatic anterior translation does not occur without distraction, and facet dislocation or fracture-dislocation should be evident. Greater than a 2-mm offset of the lamina of C2 from the C1–C3 spinolaminar line (Swischuk line) is used to distinguish traumatic subluxation from pseudosubluxation at C2-C3 in pediatric patients. In adults, translation injury at any motion segment of the cervical spine will result in spinolaminar line incongruity.

Unilateral locked facets usually cause less than 50% anterior translation of the rostral vertebral body, whereas bilateral facet dislocations result in 50% or more translation (97). Lateral mass fracture-separations (ie, floating lateral mass) (95) can cause translation or rotation (Fig 12), and bilateral pedicle fractures can result in translation morphology.

Rotational injuries can often be diagnosed on axial images and can also be appreciated on sagittal reconstructions as altered alignment of the midline sagittal plane at the injured level (93) (Fig 12b, 12c). Although the C7-T1 segment has received great attention because of the high rate of misses at this level on radiographs, it accounts for only 17% of all subaxial injuries (5,8). Most flexion-distraction and translation injuries occur at the C5-C6 and C6-C7 motion segments, where the fulcrum is located.

Teaching Point

Flexion teardrop fractures and quadrangular fractures are morphologic descriptors that really imply an injury pattern in which there is severe disruption of both posterior and anterior discoligamentous support structures, which results in severe instability, usually with complete neurologic injury (95) (Fig 13). The rostral vertebral body fractures anteroinferiorly (ie, teardrop fragment) or anteriorly (ie, quadrangular fragment). Because both the dissociated vertebral body and the facets lose their ligamentous support, the vertebra displaces posteriorly into the canal, and retrolisthesis with canal compromise is usually seen (95). Associated sagittally oriented vertebral body split fractures (Fig 13b) and facet or laminar fractures are common.

SLIC Discoligamentous Complex Score

The term *discoligamentous complex* is a new term introduced by the authors of the SLIC system; the term refers to *(a)* the anterior longitudinal ligament, intervertebral disk, and posterior longitudinal ligament anteriorly and *(b)* the ligamentum flavum, facet capsules, interspinous ligament, and supraspinous ligament posteriorly. The integrity of the capsular and ligamentous structures is strongly correlated with stability. In the SLIC system, the discoligamentous complex is graded as intact (score of 0), indeterminate (score of 1), or disrupted (score of 2). Discoligamentous complex injury and bone injury are independent predictors of outcome; however, there is inherent overlap in the scoring system because abnormal bone relationships described in the morphology score are absolute indicators of discoligamentous complex injury; for instance, the capsules must be injured in the presence of facet subluxation or widening (discoligamentous complex score of 2). Teaching Point Abnormal bone relationships at CT are the primary way that discoligamentous complex injuries are diagnosed initially.

Distraction injuries, although given a score of 3 on the basis of morphology, receive another 2 points for discoligamentous complex injury and are therefore surgical. An indeterminate score of 1 is assigned only for cases in which bone relationships are normal but abnormal T2 signal intensity is seen in the capsules or ligaments at subsequent MR imaging. An indeterminate score may also be given when isolated interspinous widening is seen at CT, because the interspinous ligament is the weakest support structure, and its integrity plays a small role in overall stability. Although a score of 1 was meant to be used infrequently, Vaccaro et al (3) reported that it was used in 30% of cases. Because of the indeterminate designation, the discoligamentous complex is the least accurate of the three SLIC components. Whether indeter-

Table 7: Cutoff Values for Hyperflexion-Distraction, Rotation, and Translation Injuries of the Subaxial Cervical Spine

Hyperflexion-distraction
Overlap of facet articular surfaces < 50%
Facet diastasis > 2 mm
Posterior disk space widening with angulation >11°
Rotation
Listhesis > 3.5 mm but <50% of caudal vertebral body width
Translation
Listhesis > 3.5 mm, usually >50% of caudal vertebral body width

Figure 10. Extension-distraction injury. Sagittal multiplanar reformatted CT image of a 61-year-old patient after a fall from standing shows a "hyperextension teardrop" fracture (arrow) off the anterior inferior lip of C2, with associated posterior spinous process fractures of C6-T1.

Figure 11. Translation injuries. **(a)** Coronal posterior volume-rendered CT image of an 85-year-old patient after an MVC shows bilateral locked facets (arrows) at C5-C6. **(b)** Sagittal "virtual radiograph" volume-rendered CT image of a 24-year-old patient who was an unrestrained backseat passenger in an MVC shows locked facets at C5 (white arrow) on C6 (black arrow), with greater than 50% translation of the C5 vertebral body. **(c)** For comparison, this sagittal volume-rendered CT image obtained with the "virtual radiograph" template shows normal alignment of the subaxial spinal lines: the anterior marginal line (yellow), the posterior marginal line (green), the spinolaminar line (blue), and the posterior spinous line (red).

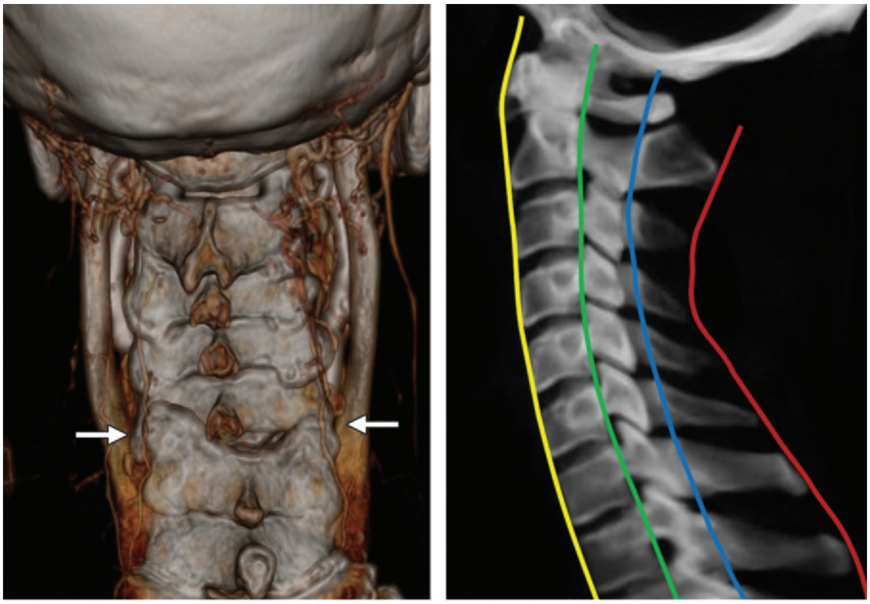

a. c.

b.

minate discoligamentous complex injuries can still result in progressive instability is a matter of controversy and remains at the core of the debate about whether adjuvant MR imaging is needed for cervical spine clearance.

SLIC Neurology Score

Neurologic injury is graded from 1 to 4, with root injuries receiving a score of 1, complete cord injuries a score of 2, incomplete cord injuries a score of 3, and incomplete cord injuries with ongoing cord compression a score of 4. The highest priority is given to incomplete injuries because the patient's clinical outcome can be altered considerably with surgical intervention. Neurologic injury may be the most important predictor of treatment (95) but is often masked in polytrauma patients with obtundation. Incomplete injuries may also be confounded by reversible spinal shock.

A burst fracture (morphology score of 2) with ongoing spinal cord compression (neurology score of 4) from retropulsion of a fragment is a classic example in which neurologic findings dictate the need for surgery, even though there may be no ligamentous instability (discoligamentous complex score of 0) (5) (Fig 8). In another example, an elderly patient may develop central cord syndrome with ongoing compression of a swollen cord by a narrowed spondylotic canal (Fig 14). There may be no evidence of discoligamentous injury at CT, but cord injury may be appreciated at MR imaging. Even though bone and ligaments may not be disrupted, a neurology score of 4 and a total SLIC score of at least 4 would be assigned. An indeterminate score of 4 reflects the varying opinions among spine surgeons as to whether decompression in this setting is necessary.

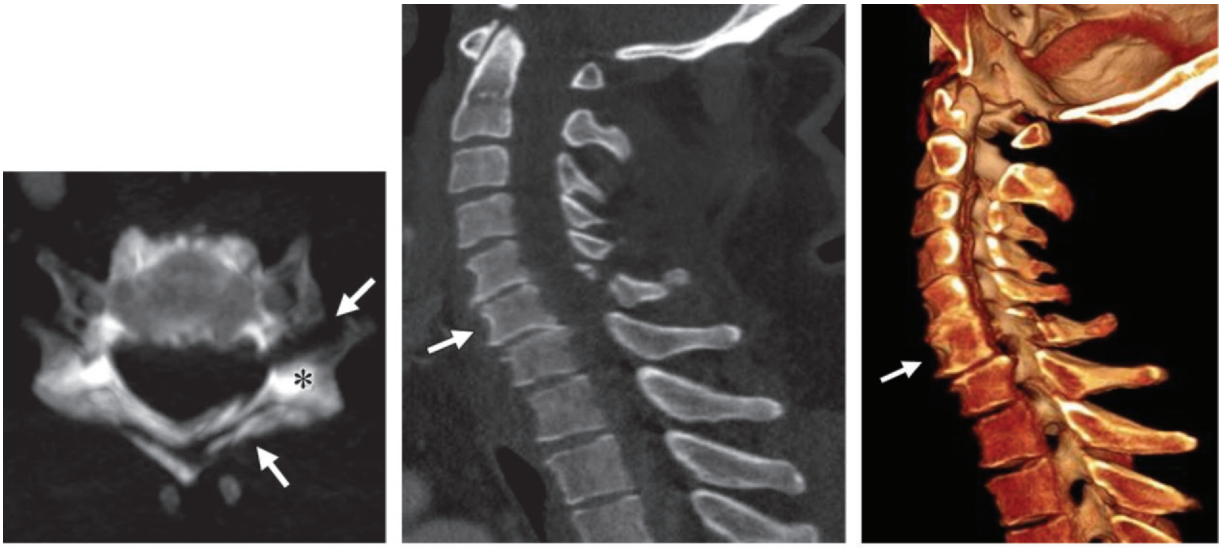

a. b. c.

Figure 12. Translation injuries: rotation-translation injury in a 61-year-old patient who was an unrestrained driver in an MVC. **(a)** Axial MIP image shows left C6 pedicle and laminar fractures (arrows), with separation of the lateral mass (*). **(b)** Multiplanar reformatted CT image through the midsagittal plane of the spine below the injured segment shows off-center spinous processes of C2 through C6 (arrow). **(c)** Sagittal half-space slab volume-rendered CT image shows less than 50% anterior translation of the C6 vertebral body, with rotated vertebral bodies at and above the injured level (arrow).

SLIC Modifiers

A number of preexisting conditions affecting the spine may influence management decisions. These conditions include underlying severe spondylosis, diffuse idiopathic skeletal hyperostosis, prior surgery, osteoporosis, posterior longitudinal ligament ossification, rheumatoid arthritis, and ankylosing spondylitis. Spinal fracture in ankylosing spondylitis causes the portions of the spine that are located cephalad and caudad to the injury to behave as long lever arms. These fractures may be subtle initially but are extremely unstable (5).

Limitations of Multidetector CT

Although multidetector CT is often sufficient for making the binary determination of whether surgery is necessary or not, important determinants of management, including disk herniations, ligamentum flavum infolding, cord swelling, contusion or hemorrhage, and epidural hematoma, are not well evaluated with CT but are clearly depicted at MR imaging (98). MR imaging is also often performed before closed reduction because disk herniations in this setting may worsen neurologic injury (5,99). MR imaging plays an important role in planning whether an anterior or posterior surgical approach is needed, because diskectomy may be necessary for traumatic disk herniation.

Normal Variants and Pitfalls

Congenital defects may occasionally predispose patients to injury disproportionate to the severity of the injury mechanism and may be confused with fractures or dislocations (100). Congenital absence of the posterior arches may occur (101,102) (Fig 15a). Absence of the anterior arch or pedicles can also be seen, although both are rare (100).

Typically, congenital clefts are smooth and well corticated, whereas fractures are sharp and nonsclerotic. In the atlas, congenital clefts occur posteriorly at a rate of 4% and anteriorly at a rate of 0.1% (103) (Fig 15b). Osseous clefts may also occur at the anterior margins of the transverse foramina (Fig 4b).

Os odontoideum can potentially be confused with fracture and is a source of instability (104). The consensus is increasing that os odontoideum is caused by trauma in childhood, rather than being a congenital anomaly (102). Os odontoideum is distinguished from os terminale, a secondary ossification center at the odontoid tip, by its large size, and os odontoideum is distinguished from a chronic type II fracture of a fully developed odontoid by the presence of a large gap separating the os odontoideum from the axis body (Fig 16). Os odontoideum is often treated surgically and should be mentioned when found incidentally.

Partial ossification of the atlanto-occipital membrane is relatively common and can be a source of diagnostic confusion. This ossification may appear as a well-corticated bone fragment posterior to the lateral mass of the atlas (102) or can manifest as a bone excrescence termed *ponticulus posticus* (Latin for little posterior bridge)

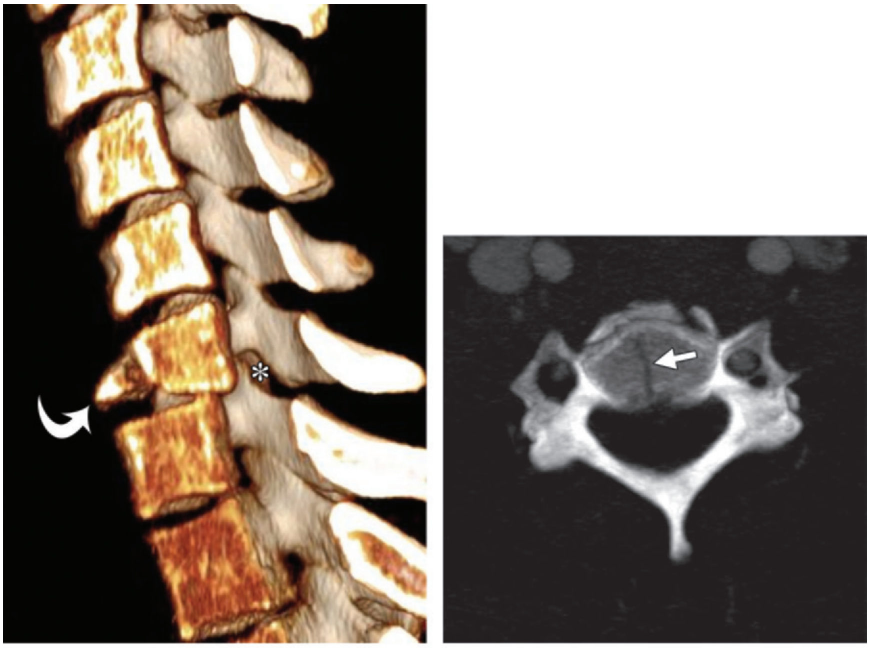

a. b.

Figure 13. Translation injuries: flexion teardrop injury in a 27-year-old woman who was a victim of assault. **(a)** Sagittal half-space slab volume-rendered CT image shows the flexion teardrop injury pattern, with the classic findings of a triangular fragment (arrow) off the anterior inferior C6 vertebral body and posterior translation of the vertebral body and posterior elements, resulting in facet widening (*). **(b)** Axial MIP image shows a sagittal fracture line (arrow) through the C6 vertebral body posterior to the teardrop fragment.

Figure 14. Neurologic injury without discoligamentous injury in a 95-year-old patient after a fall from standing. Sagittal multiplanar reformatted CT image shows a spondylotic spine with fractures of the tips of the C5 and C6 spinous processes (arrow). There were no other fractures or evidence of ligament injury. Clinically, the patient had central cord syndrome, and at MR imaging, cord edema was depicted (not shown). Surgical decompression was performed on the basis of the neurologic injury.

partially covering the horizontally oriented vertebral artery. When the excrescence completely surrounds the vertebral artery, it is called an arcuate foramen (Fig 15c) (102).

Conclusions

Multidetector CT has become the standard of care as the initial screening examination for evaluating blunt cervical spine trauma in patients who do not meet criteria for clinical clearance. In addition to being able to recognize and accurately communicate the wide spectrum of craniocervical junction and subaxial cervical spine injuries seen at multidetector CT, radiologists can provide added value to their trauma and spine surgery colleagues by developing a working knowledge of both well-established and newly introduced grading systems and their implications for patient management.

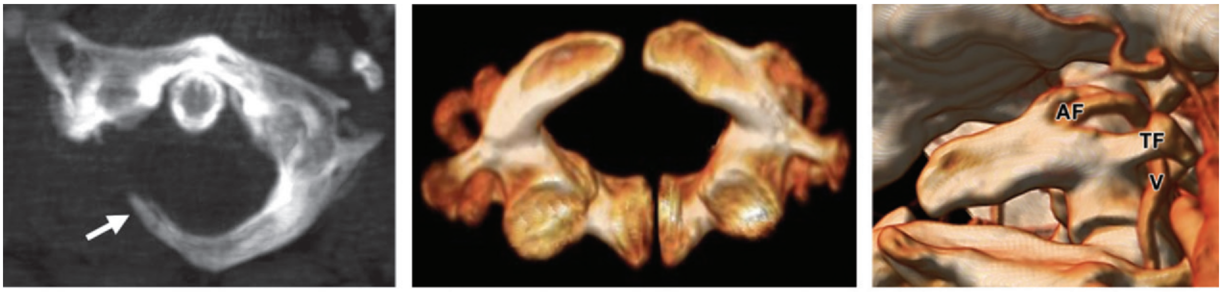

a. b. c.

Figure 15. Congenital anomalies in a 50-year-old man with a type II dens fracture after a bodysurfing accident. **(a)** Axial MIP image of the atlas shows a congenital defect involving a portion of the right posterior arch. The tip of the developed portion of the right posterior arch is fractured (arrow). **(b)** Volume-rendered CT image of the atlas with anterior and posterior congenital clefts. The atlas has been virtually disarticulated by using the mask function. **(c)** Volume-rendered CT image of the atlas shows the vertebral artery *(V)* coursing through the right transverse foramen *(TF)* and entering a right arcuate foramen *(AF)*.

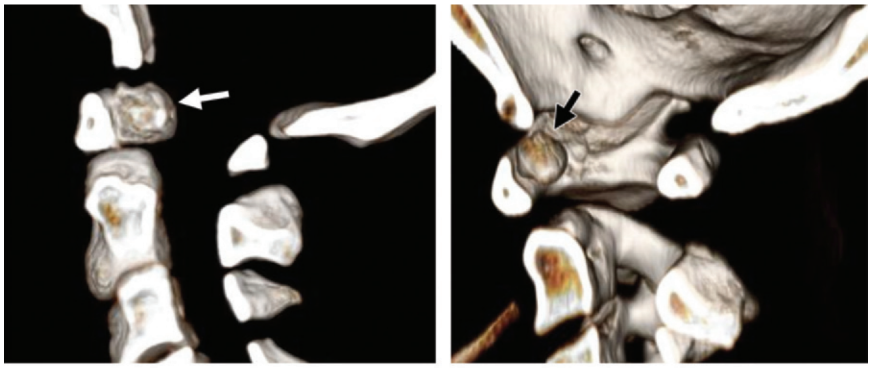

a. b.

Figure 16. Old odontoid fracture compared with os odontoideum. **(a)** Half-space slab volume-rendered CT image of a 61-year-old patient struck with a brick in the back of the head shows an old unfused odontoid fracture with a short gap between the odontoid and the C2 body, which maintains the basic shape of the dens (arrow). **(b)** Half-space slab volume-rendered CT image of a 9-year-old patient shows an os odontoideum (arrow). Note the large gap between the os odontoideum and the axis body.

References

1. Berkowitz M. Assessing the socioeconomic impact of improved treatment of head and spinal cord injuries. J Emerg Med 1993;11(suppl 1):63–67.
2. Bracken MB, Freeman DH Jr, Hellenbrand K. Incidence of acute traumatic hospitalized spinal cord injury in the United States, 1970-1977. Am J Epidemiol 1981;113(6):615–622.
3. Vaccaro AR, Hulbert RJ, Patel AA, et al. The subaxial cervical spine injury classification system: a novel approach to recognize the importance of morphology, neurology, and integrity of the disco-ligamentous complex. Spine (Phila Pa 1976) 2007;32(21): 2365–2374.
4. Vaccaro AR, An HS, Lin S, Sun S, Balderston RA, Cotler JM. Noncontiguous injuries of the spine. J Spinal Disord 1992;5(3):320–329.
5. Kwon BK, Vaccaro AR, Grauer JN, Fisher CG, Dvorak MF. Subaxial cervical spine trauma. J Am Acad Orthop Surg 2006;14(2):78–89.
6. American College of Surgeons. Advanced Trauma Life Support (ATLS®) student course manual. 9th ed. Chicago, Ill: American College of Surgeons, 2012.
7. Stiell IG, Wells GA, Vandemheen KL, et al. The Canadian C-spine rule for radiography in alert and stable trauma patients. JAMA 2001;286(15): 1841–1848.
8. Hoffman JR, Mower WR, Wolfson AB, Todd KH, Zucker MI. Validity of a set of clinical criteria to rule out injury to the cervical spine in patients with blunt trauma. National Emergency X-Radiography Utilization Study Group. N Engl J Med 2000;343 (2):94–99.
9. American College of Radiology. ACR Appropriateness Criteria®: suspected spine trauma. Reston, Va: American College of Radiology, 2012.
10. Rose MK, Rosal LM, Gonzalez RP, et al. Clinical clearance of the cervical spine in patients with distracting injuries: it is time to dispel the myth. J Trauma Acute Care Surg 2012;73(2):498–502.
11. Blackmore CC, Emerson SS, Mann FA, Koepsell TD. Cervical spine imaging in patients with trauma: determination of fracture risk to optimize use. Radiology 1999;211(3):759–765.
12. Morris CG, McCoy É. Clearing the cervical spine in unconscious polytrauma victims, balancing

risks and effective screening. Anaesthesia 2004;59 (5):464–482.
13. Reid DC, Henderson R, Saboe L, Miller JD. Etiology and clinical course of missed spine fractures. J Trauma 1987;27(9):980–986.
14. Stelfox HT, Velmahos GC, Gettings E, Bigatello LM, Schmidt U. Computed tomography for early and safe discontinuation of cervical spine immobilization in obtunded multiply injured patients. J Trauma 2007;63(3):630–636.
15. Nuñez DB Jr, Ahmad AA, Coin CG, et al. Clearing the cervical spine in multiple trauma victims: a time-effective protocol using helical computed tomography. Emerg Radiol 1994;1(6):273–278.
16. Theocharopoulos NC, Chatzakis G, Damilakis J. Is radiography justified for the evaluation of patients presenting with cervical spine trauma? Med Phys 2009;36(10):4461–4470.
17. Kirschner J, Seupaul RA. Does computed tomography rule out clinically significant cervical spine injuries in obtunded or intubated blunt trauma patients? [corrected]. Ann Emerg Med 2012;60(6):737–738. [Published correction appears in Ann Emerg Med 2013;61(2):261.]
18. Muchow RD, Resnick DK, Abdel MP, Munoz A, Anderson PA. Magnetic resonance imaging (MRI) in the clearance of the cervical spine in blunt trauma: a meta-analysis. J Trauma 2008;64(1):179–189.
19. Panczykowski DM, Tomycz ND, Okonkwo DO. Comparative effectiveness of using computed tomography alone to exclude cervical spine injuries in obtunded or intubated patients: meta-analysis of 14,327 patients with blunt trauma. J Neurosurg 2011;115(3):541–549.
20. British Trauma Society. Guidelines for the initial management and assessment of spinal injury: British Trauma Society, 2002. Injury 2003;34(6):405–425.
21. Hogan GJ, Mirvis SE, Shanmuganathan K, Scalea TM. Exclusion of unstable cervical spine injury in obtunded patients with blunt trauma: is MR imaging needed when multi–detector row CT findings are normal? Radiology 2005;237(1):106–113.
22. Como JJ, Thompson MA, Anderson JS, et al. Is magnetic resonance imaging essential in clearing the cervical spine in obtunded patients with blunt trauma? J Trauma 2007;63(3):544–549.
23. Tomycz ND, Chew BG, Chang YF, et al. MRI is unnecessary to clear the cervical spine in obtunded/comatose trauma patients: the four-year experience of a level I trauma center. J Trauma 2008;64(5):1258–1263.
24. Stassen NA, Williams VA, Gestring ML, Cheng JD, Bankey PE. Magnetic resonance imaging in combination with helical computed tomography provides a safe and efficient method of cervical spine clearance in the obtunded trauma patient. J Trauma 2006;60(1):171–177.
25. Sarani B, Waring S, Sonnad S, Schwab CW. Magnetic resonance imaging is a useful adjunct in the evaluation of the cervical spine of injured patients. J Trauma 2007;63(3):637–640.
26. Sliker CW. Blunt cerebrovascular injuries: imaging with multidetector CT angiography. RadioGraphics 2008;28(6):1689–1708; discussion 1709–1710.
27. Burlew CC, Biffl WL, Moore EE, Barnett CC, Johnson JL, Bensard DD. Blunt cerebrovascular injuries: redefining screening criteria in the era of noninvasive diagnosis. J Trauma Acute Care Surg 2012;72 (2):330–335; discussion 336–337.
28. Schneidereit NP, Simons R, Nicolaou S, et al. Utility of screening for blunt vascular neck injuries with computed tomographic angiography. J Trauma 2006;60(1):209–215; discussion 215–216.
29. Cothren CC, Moore EE, Ray CE Jr, et al. Screening for blunt cerebrovascular injuries is cost-effective. Am J Surg 2005;190(6):845–849.
30. DiCocco JM, Emmett KP, Fabian TC, Zarzaur BL, Williams JS, Croce MA. Blunt cerebrovascular injury screening with 32-channel multidetector computed tomography: more slices still don't cut it. Ann Surg 2011;253(3):444–450.
31. Goodwin RB, Beery PR 2nd, Dorbish RJ, et al. Computed tomographic angiography versus conventional angiography for the diagnosis of blunt cerebrovascular injury in trauma patients. J Trauma 2009;67(5):1046–1050.
32. Anderson SW, Soto JA, Lucey BC, Burke PA, Hirsch EF, Rhea JT. Blunt trauma: feasibility and clinical utility of pelvic CT angiography performed with 64–detector row CT. Radiology 2008;246(2):410–419.
33. Sliker CW, Shanmuganathan K, Mirvis SE. Diagnosis of blunt cerebrovascular injuries with 16-MDCT: accuracy of whole-body MDCT compared with neck MDCT angiography. AJR Am J Roentgenol 2008;190(3):790–799.
34. Junewick JJ. Pediatric craniocervical junction injuries. AJR Am J Roentgenol 2011;196(5):1003–1010.
35. Chang W, Alexander MT, Mirvis SE. Diagnostic determinants of craniocervical distraction injury in adults. AJR Am J Roentgenol 2009;192(1):52–58.
36. Deliganis AV, Baxter AB, Hanson JA, et al. Radiologic spectrum of craniocervical distraction injuries. RadioGraphics 2000;20(Spec Issue):S237–S250. [Published correction appears in RadioGraphics 2001;21(2):520.]
37. Rojas CA, Bertozzi JC, Martinez CR, Whitlow J. Reassessment of the craniocervical junction: normal values on CT. AJNR Am J Neuroradiol 2007; 28(9):1819–1823.
38. Horn EM, Feiz-Erfan I, Lekovic GP, Dickman CA, Sonntag VK, Theodore N. Survivors of occipitoatlantal dislocation injuries: imaging and clinical correlates. J Neurosurg Spine 2007;6(2):113–120.
39. Papadopoulos SM, Dickman CA, Sonntag VK, Rekate HL, Spetzler RF. Traumatic atlantooccipital dislocation with survival. Neurosurgery 1991; 28(4):574–579.
40. Goradia D, Blackmore CC, Talner LB, Bittles M, Meshberg E. Predicting radiology resident errors in diagnosis of cervical spine fractures. Acad Radiol 2005;12(7):888–893.
41. Chaput CD, Walgama J, Torres E, et al. Defining and detecting missed ligamentous injuries of the occipitocervical complex. Spine (Phila Pa 1976) 2011; 36(9):709–714.
42. Powers B, Miller MD, Kramer RS, Martinez S, Gehweiler JA Jr. Traumatic anterior atlanto-occipital dislocation. Neurosurgery 1979;4(1):12–17.
43. Dziurzynski K, Anderson PA, Bean DB, et al. A blinded assessment of radiographic criteria for atlanto-occipital dislocation. Spine (Phila Pa 1976) 2005;30(12):1427–1432.
44. Harris JH Jr, Carson GC, Wagner LK, Kerr N. Radiologic diagnosis of traumatic occipitovertebral dissociation. II. Comparison of three methods of detecting occipitovertebral relationships on lateral radiographs of supine subjects. AJR Am J Roentgenol 1994;162(4):887–892.

45. Hinck VC, Hopkins CE. Measurement of the atlanto-dental interval in the adult. Am J Roentgenol Radium Ther Nucl Med 1960;84:945–951.
46. Gonzalez LF, Fiorella D, Crawford NR, et al. Vertical atlantoaxial distraction injuries: radiological criteria and clinical implications. J Neurosurg Spine 2004;1(3):273–280.
47. Radcliff KE, Ben-Galim P, Dreiangel N, et al. Comprehensive computed tomography assessment of the upper cervical anatomy: what is normal? Spine J 2010;10(3):219–229. doi:10.1016/j.spinee.2009.12.021.
48. el-Khoury GY, Kathol MH, Daniel WW. Imaging of acute injuries of the cervical spine: value of plain radiography, CT, and MR imaging. AJR Am J Roentgenol 1995;164(1):43–50.
49. Radcliff K, Kepler C, Reitman C, Harrop J, Vaccaro A. CT and MRI-based diagnosis of craniocervical dislocations: the role of the occipitoatlantal ligament. Clin Orthop Relat Res 2012;470(6):1602–1613.
50. Leone A, Cerase A, Colosimo C, Lauro L, Puca A, Marano P. Occipital condylar fractures: a review. Radiology 2000;216(3):635–644.
51. Hanson JA, Deliganis AV, Baxter AB, et al. Radiologic and clinical spectrum of occipital condyle fractures: retrospective review of 107 consecutive fractures in 95 patients. AJR Am J Roentgenol 2002;178(5):1261–1268.
52. Malham GM, Ackland HM, Jones R, Williamson OD, Varma DK. Occipital condyle fractures: incidence and clinical follow-up at a level 1 trauma centre. Emerg Radiol 2009;16(4):291–297.
53. Anderson PA, Montesano PX. Morphology and treatment of occipital condyle fractures. Spine (Phila Pa 1976) 1988;13(7):731–736.
54. Gehweiler JA Jr, Duff DE, Martinez S, Miller MD, Clark WM. Fractures of the atlas vertebra. Skeletal Radiol 1976;1(2):97–102.
55. Anderson LD, D'Alonzo RT. Fractures of the odontoid process of the axis. J Bone Joint Surg Am 1974;56(8):1663–1674.
56. Effendi B, Roy D, Cornish B, Dussault RG, Laurin CA. Fractures of the ring of the axis: a classification based on the analysis of 131 cases. J Bone Joint Surg Br 1981;63-B(3):319–327.
57. Levine AM, Edwards CC. The management of traumatic spondylolisthesis of the axis. J Bone Joint Surg Am 1985;67(2):217–226.
58. Fielding JW, Hawkins RJ. Atlanto-axial rotatory fixation (fixed rotatory subluxation of the atlanto-axial joint). J Bone Joint Surg Am 1977;59(1):37–44.
59. Tuli S, Tator CH, Fehlings MG, Mackay M. Occipital condyle fractures. Neurosurgery 1997;41(2):368–376; discussion 376–377.
60. Kakarla UK, Chang SW, Theodore N, Sonntag VK. Atlas fractures. Neurosurgery 2010;66(suppl 3):60–67.
61. Fowler JL, Sandhu A, Fraser RD. A review of fractures of the atlas vertebra. J Spinal Disord 1990;3(1):19–24.
62. Levine AM, Edwards CC. Fractures of the atlas. J Bone Joint Surg Am 1991;73(5):680–691.
63. Spence KF Jr, Decker S, Sell KW. Bursting atlantal fracture associated with rupture of the transverse ligament. J Bone Joint Surg Am 1970;52(3):543–549.
64. Dickman CA, Greene KA, Sonntag VK. Injuries involving the transverse atlantal ligament: classification and treatment guidelines based upon experience with 39 injuries. Neurosurgery 1996;38(1):44–50.
65. Heller JG, Viroslav S, Hudson T. Jefferson fractures: the role of magnification artifact in assessing transverse ligament integrity. J Spinal Disord 1993;6(5):392–396.
66. Greene KA, Dickman CA, Marciano FF, Drabier JB, Hadley MN, Sonntag VK. Acute axis fractures: analysis of management and outcome in 340 consecutive cases. Spine (Phila Pa 1976) 1997;22(16):1843–1852.
67. Pryputniewicz DM, Hadley MN. Axis fractures. Neurosurgery 2010;66(suppl 3):68–82.
68. Lakshmanan P, Jones A, Howes J, Lyons K. CT evaluation of the pattern of odontoid fractures in the elderly: relationship to upper cervical spine osteoarthritis. Eur Spine J 2005;14(1):78–83.
69. Julien TD, Frankel B, Traynelis VC, Ryken TC. Evidence-based analysis of odontoid fracture management. Neurosurg Focus 2000;8(6):e1. http://thejns.org/doi/pdfplus/10.3171/foc.200 0.8.6.2. Accessed September 1, 2013.
70. Traynelis VC. Evidence-based management of type II odontoid fractures. Clin Neurosurg 1997;44:41–49.
71. Hadley MN, Browner C, Sonntag VK. Axis fractures: a comprehensive review of management and treatment in 107 cases. Neurosurgery 1985;17(2):281–290.
72. Dunn ME, Seljeskog EL. Experience in the management of odontoid process injuries: an analysis of 128 cases. Neurosurgery 1986;18(3):306–310.
73. Ekong CE, Schwartz ML, Tator CH, Rowed DW, Edmonds VE. Odontoid fracture: management with early mobilization using the halo device. Neurosurgery 1981;9(6):631–637.
74. Lennarson PJ, Mostafavi H, Traynelis VC, Walters BC. Management of type II dens fractures: a case-control study. Spine (Phila Pa 1976) 2000;25(10):1234–1237.
75. Hadley MN, Browner CM, Liu SS, Sonntag VK. New subtype of acute odontoid fractures (type IIA). Neurosurgery 1988;22(1 pt 1):67–71.
76. Koivikko MP, Kiuru MJ, Koskinen SK. Occurrence of comminution (type IIA) in type II odontoid process fractures: a multi-slice CT study. Emerg Radiol 2003;10(2):84–86.
77. Traynelis VC, Marano GD, Dunker RO, Kaufman HH. Traumatic atlanto-occipital dislocation: case report. J Neurosurg 1986;65(6):863–870.
78. Wood-Jones F. The ideal lesion produced by judicial hanging. Lancet 1913;4662:53. http://www.sciencedirect.com/science/article/pii/S0140673601477828. Published January 1913. Accessed September 1, 2013. doi:10.1016/S0140-6736(01)47782-8.
79. Schneider RC, Livingston KE, Cave AJ, Hamilton G. "Hangman's fracture" of the cervical spine. J Neurosurg 1965;22:141–154.
80. Burke JT, Harris JH Jr. Acute injuries of the axis vertebra. Skeletal Radiol 1989;18(5):335–346.
81. Mirvis SE, Young JW, Lim C, Greenberg J. Hangman's fracture: radiologic assessment in 27 cases. Radiology 1987;163(3):713–717.

82. Suchomel P, Choutka O. Miscellaneous C2 fractures. Berlin, Germany: Springer Verlag, 2011.
83. Roche CJ, O'Malley M, Dorgan JC, Carty HM. A pictorial review of atlanto-axial rotatory fixation: key points for the radiologist. Clin Radiol 2001;56(12):947–958.
84. Roche CJ, King SJ, Dangerfield PH, Carty HM. The atlanto-axial joint: physiological range of rotation on MRI and CT. Clin Radiol 2002;57(2):103–108.
85. Johnson DP, Fergusson CM. Early diagnosis of atlanto-axial rotatory fixation. J Bone Joint Surg Br 1986;68(5):698–701.
86. Allen BL Jr, Ferguson RL, Lehmann TR, O'Brien RP. A mechanistic classification of closed, indirect fractures and dislocations of the lower cervical spine. Spine (Phila Pa 1976) 1982;7(1):1–27.
87. Aarabi B, Walters BC, Dhall SS, et al. Subaxial cervical spine injury classification systems. Neurosurgery 2013;72(suppl 2):170–186.
88. Harris JH Jr, Edeiken-Monroe B, Kopaniky DR. A practical classification of acute cervical spine injuries. Orthop Clin North Am 1986;17(1):15–30.
89. Shono Y, McAfee PC, Cunningham BW. The pathomechanics of compression injuries in the cervical spine: nondestructive and destructive investigative methods. Spine (Phila Pa 1976) 1993;18(14):2009–2019.
90. Anderson PA, Moore TA, Davis KW, et al. Cervical spine injury severity score: assessment of reliability. J Bone Joint Surg Am 2007;89(5):1057–1065.
91. Stone AT, Bransford RJ, Lee MJ, et al. Reliability of classification systems for subaxial cervical injuries. Evid Based Spine Care J 2010;1(3):19–26.
92. Moore TA, Vaccaro AR, Anderson PA. Classification of lower cervical spine injuries. Spine (Phila Pa 1976) 2006;31(suppl 11):S37–S43; discussion S61.
93. Vaccaro AR, Lehman RAJ Jr, Hurlbert RJ, et al. A new classification of thoracolumbar injuries: the importance of injury morphology, the integrity of the posterior ligamentous complex, and neurologic status. Spine (Phila Pa 1976) 2005;30(20):2325–2333.
94. Patel AA, Dailey A, Brodke DS, et al. Subaxial cervical spine trauma classification: the Subaxial Injury Classification system and case examples. Neurosurg Focus 2008;25(5):E8. http://thejns.org/doi/pdf/10.3171/FOC.2008.25.11.E8. Accessed September 1, 2013
95. Dvorak MF, Fisher CG, Fehlings MG, et al. The surgical approach to subaxial cervical spine injuries: an evidence-based algorithm based on the SLIC classification system. Spine (Phila Pa 1976) 2007;32(23):2620–2629.
96. Edeiken-Monroe BW, Wagner LK, Harris JH Jr. Hyperextension dislocation of the cervical spine. AJR Am J Roentgenol 1986;146(4):803–808.
97. Braakman R, Vinken PJ. Unilateral facet interlocking in the lower cervical spine. J Bone Joint Surg Br 1967;49(2):249–257.
98. Miyanji F, Furlan JC, Aarabi B, Arnold PM, Fehlings MG. Acute cervical traumatic spinal cord injury: MR imaging findings correlated with neurologic outcome—prospective study with 100 consecutive patients. Radiology 2007;243(3):820–827.
99. Vaccaro AR, Falatyn SP, Flanders AE, Balderston RA, Northrup BE, Cotler JM. Magnetic resonance evaluation of the intervertebral disc, spinal ligaments, and spinal cord before and after closed traction reduction of cervical spine dislocations. Spine (Phila Pa 1976) 1999;24(12):1210–1217.
100. Mellado JM, Larrosa R, Martín J, Yanguas N, Solanas S, Cozcolluela MR. MDCT of variations and anomalies of the neural arch and its processes. II. Articular processes, transverse processes, and high cervical spine. AJR Am J Roentgenol 2011;197(1):W114–W121. http://www.ajronline.org/doi/pdf/10.2214/AJR.10.5811. Accessed September 1, 2013.
101. Sharma A, Gaikwad SB, Deol PS, Mishra NK, Kale SS. Partial aplasia of the posterior arch of the atlas with an isolated posterior arch remnant: findings in three cases. AJNR Am J Neuroradiol 2000;21(6):1167–1171.
102. Carr RB, Fink KR, Gross JA. Imaging of trauma. I. Pseudotrauma of the spine—osseous variants that may simulate injury. AJR Am J Roentgenol 2012;199(6):1200–1206.
103. Geipel P. Studies on the fissure formation of the atlas and epistropheus. IV [in German]. Zentralbl Allg Pathol 1955;94(1-2):19–84.
104. Klimo P Jr, Kan P, Rao G, Apfelbaum R, Brockmeyer D. Os odontoideum: presentation, diagnosis, and treatment in a series of 78 patients. J Neurosurg Spine 2008;9(4):332–342.

Multidetector CT of Blunt Cervical Spine Trauma in Adults

David Dreizin, MD • Michael Letzing, MD • Clint W. Sliker, MD • Falgun H. Chokshi, MD • Uttam Bodanapally, MD • Stuart E. Mirvis, MD • Robert M. Quencer, MD • Felipe Munera, MD

RadioGraphics 2014; 34:1842–1865 • **Published online** 10.1148/rg.347130094 • **Content Codes:** CT ER MK NR

Page 1843
Clearance of the cervical spine on clinical grounds alone has become the standard of care in alert adult patients with no midline cervical tenderness, neurologic symptoms, or distracting injuries.

Page 1855
The three components of SLIC are *(a)* morphologic findings of bone spinal column disruption, *(b)* the integrity of the discoligamentous complex, and *(c)* neurologic status (95). The three scores for these three components are summed to give the SLIC score (total score). Combined scores of 5 or more indicate the need for surgical intervention. Injuries with scores of 3 or less can be managed without surgery, and scores of 4 are indeterminate.

Page 1856
Fragments with a triangular teardrop morphology should still be characterized as compression injury with a score of 1 or 2 if there is no associated posterior element distraction or vertebral body translation.

Page 1858
Flexion teardrop fractures and quadrangular fractures are morphologic descriptors that really imply an injury pattern in which there is severe disruption of both posterior and anterior discoligamentous support structures, which results in severe instability, usually with complete neurologic injury (95) (Fig 13). The rostral vertebral body fractures anteroinferiorly (ie, teardrop fragment) or anteriorly (ie, quadrangular fragment). Because both the dissociated vertebral body and the facets lose their ligamentous support, the vertebra displaces posteriorly into the canal, and retrolisthesis with canal compromise is usually seen (95).

Page 1858
Abnormal bone relationships at CT are the primary way that discoligamentous complex injuries are diagnosed initially.